Article

Slow Anion Exchange, Conformational Equilibria, and Fluorescent Sensing in Venus Flytrap Aminopyridinium-Based Anion Hosts

Karl J. Wallace, Warwick J. Belcher, David R. Turner, Kauser F. Syed, and Jonathan W. Steed

J. Am. Chem. Soc., **2003**, 125 (32), 9699-9715• DOI: 10.1021/ja034921w • Publication Date (Web): 17 July 2003

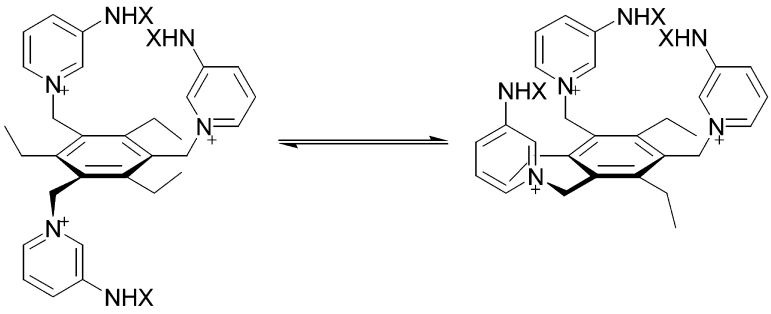

More About This Article

Additional resources and features associated with this article are available within the HTML version:

- Supporting Information
- Links to the 21 articles that cite this article, as of the time of this article download
- Access to high resolution figures
- Links to articles and content related to this article
- Copyright permission to reproduce figures and/or text from this article

View the Full Text HTML

J|A|C|S
ARTICLES
Published on Web 07/17/2003

Slow Anion Exchange, Conformational Equilibria, and Fluorescent Sensing in Venus Flytrap Aminopyridinium-Based Anion Hosts

Karl J. Wallace, Warwick J. Belcher, David R. Turner, Kauser F. Syed, and Jonathan W. Steed*

Contribution from the Department of Chemistry, King's College London, Strand, London WC2R 2LS, U.K.

Received February 28, 2003; E-mail: jon.steed@kcl.ac.uk

Abstract: The synthesis, anion binding, and conformational properties of a series of 3-aminopyridinium-based, tripodal, tricationic hosts for anions are described. Slow anion and conformational exchange on the ^{1}H NMR time scale at low temperature, coupled with NMR titration, results in a high level of understanding of the anion-binding properties of the compounds, particularly with respect to significant conformational change resulting from induced fit complexation. Peak selectivity for halides, particularly Cl^-, is observed. The approach has been extended to dipodal and tripodal podands based on 3-aminopyridinium "arms" containing photoactive anthracenyl moieties. The 1,3,5-tripodal host shows a remarkable selectivity for acetate over other anions, in contrast to the analogous unsubstituted tris(3-aminopyridinium) analogue, despite the fact that low-temperature ^{1}H NMR experiments reveal a total of four acetate-binding conformations. Photodimerization of anthracene units results in the formation of potential fluorescent anion sensors.

Introduction

The design and synthesis of flexible "podand" type host molecules capable of selective guest recognition is highly topical[1−13] and has been recently reviewed.[14,15] In comparison to more rigid cyclic systems, podands are frequently more readily synthesized, can display rapid complexation/decomplexation kinetics, and may undergo significant conformational changes on binding, which may form the basis of molecular switches or switchable sensing devices.[1] Significant recent work has focused on tripodal species containing a trisubstituted triethylbenzene core.[1,2,4−6,15,16] The resulting hexasubstituted molecules exhibit a preference of some 10−15 kJ mol^{-1} for an alternating (3-up, 3-down) conformation about the central aryl ring,[2,5,15] allowing the preparation of partially preorganized tripodal hosts in which the three guest-binding arms are all orientated in the same direction and are thus able to chelate their target substrate. Anslyn et al. have used guanidinium and boronic acid derivatives, for example, as selective hosts and sensors for a variety of carboxylic acid conjugate anions found in beverages such as Gatorade and scotch.[4,6]

In the development of molecular sensors, fluorescence spectroscopy has become an important analytical technique in recent years.[17] There have been numerous receptors containing chromophores for the detection of cationic species, and the topic has been eloquently reviewed by de Silva.[18] Photoactive molecular sensors for the detection of anions have been studied less, but are of significant and growing interest.[19−22] The most common mechanism used for fluorescence studies in host−guest chemistry is via a photoinduced electron-transfer strategy (PET).

(1) Abouderbala, L. O.; Belcher, W. J.; Boutelle, M. G.; Cragg, P. J.; Steed, J. W.; Turner, D. R.; Wallace, K. J. *Proc. Natl. Acad. Sci. U.S.A.* **2002**, *99*, 5001−5006.
(2) Abouderbala, L. O.; Belcher, W. J.; Boutelle, M. G.; Cragg, P. J.; Fabre, M.; Dhaliwal, J.; Steed, J. W.; Turner, D. R.; Wallace, K. J. *Chem. Commun.* **2002**, 358−359.
(3) Lavigne, J. J.; Anslyn, E. V. *Angew. Chem., Int. Ed.* **1999**, *38*, 3666−3669.
(4) Wiskur, S. L.; Anslyn, E. V. *J. Am. Chem. Soc.* **2001**, *123*, 10109−10110.
(5) Metzger, A.; Lynch, V. M.; Anslyn, E. V. *Angew. Chem., Int. Ed. Engl.* **1997**, *36*, 862−865.
(6) Cabell, L. A.; Best, M. D.; Lavigne, J. J.; Schneider, S. E.; Perreault, D. M.; Katherine, M.-K.; Anslyn, E. V. *J. Chem. Soc., Perkin Trans. 2* **2001**, 315−323.
(7) Hartshorn, C. M.; Steel, P. J. *Angew. Chem., Int. Ed. Engl.* **1996**, *35*, 2655−2657.
(8) Choi, H. J.; Park, Y. S.; Yun, S. H.; Kim, H. S.; Cho, C. S.; Ko, K.; Ahn, K. H. *Org. Lett.* **2002**, *4*, 795−798.
(9) Sun, W.-Y.; Xie, J.; Okamura, T.-A.; Huang, C.-K.; Ueyama, N. *Chem. Commun.* **2000**, 1429−1430.
(10) Christofi, A. M.; Garratt, P. J.; Hogarth, G. *Tetrahedron* **2001**, *57*, 751−759.
(11) Garratt, P. J.; Ng, Y. F.; Steed, J. W. *Tetrahedron* **2000**, *56*, 4501−4509.
(12) Chin, J.; Walsdorff, C.; Stranix, B.; Oh, J.; Chung, H. J.; Park, S.-M.; Kim, K. *Angew. Chem., Int. Ed.* **1999**, *38*, 2756−2759.
(13) Walsdorff, C.; Saak, W.; Pohl, S. *J. Chem. Res., Synop.* **1996**, 282−283.
(14) Steed, J. W.; Wallace, K. J. In *Advances in Supramolecular Chemistry*; Gokel, G. W., Ed.; Cerberus: New York, 2003; Vol. 9, Ch. 5, pp 221−262.
(15) Hennrich, G.; Anslyn, E. V. *Chem.-Eur. J.* **2002**, *8*, 2219−2224.
(16) O'Leary, B. M.; Szabo, T.; Svenstrup, N.; Schalley, C. A.; Lützen, A.; Schäfer, M.; Rebek, J., Jr. *J. Am. Chem. Soc.* **2001**, *123*, 11519−11533.
(17) Kubo, J.; Tsukahara, M.; Ishitara, S.; Tokita, S. *Chem. Commun.* **2000**, 653−654.
(18) de Silva, A. P.; Gunaratne, H. Q. N.; Gunnlaugsson, T.; Huxley, A. J. M.; McCoy, C. P.; Rademacher, J. T.; Rice, T. E. *Chem. Rev.* **1997**, *97*, 1515−1566.
(19) Gale, P. A. *Coord. Chem. Rev.* **2001**, *213*, 79−128.
(20) Gale, P. A. *Coord. Chem. Rev.* **2000**, *199*, 181−233.
(21) Beer, P. D.; Gale, P. A. *Angew. Chem., Int. Ed.* **2001**, *40*, 487−516.
(22) Schmidtchen, F. P.; Berger, M. *Chem. Rev.* **1997**, *97*, 1609−1646.

Scheme 1. Synthesis of Aminopyridine-Based Hosts

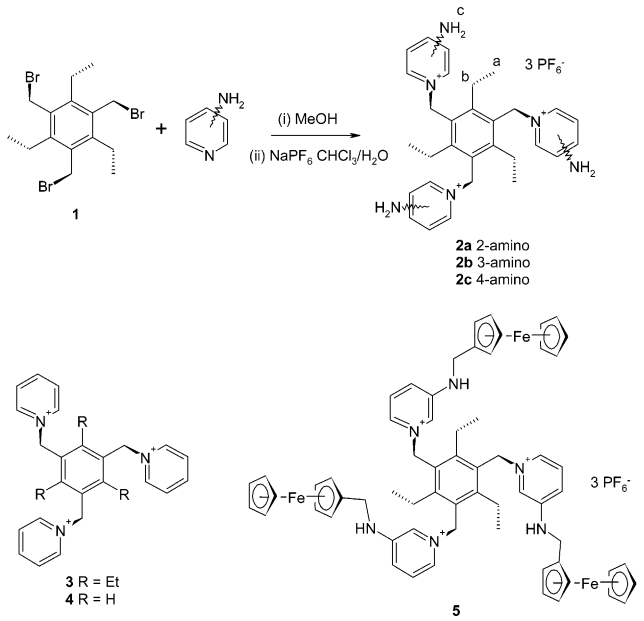

The host is made up of a fluorophore site, a receptor site, and a spacer. The PET signaling system shows either an "on−off" or an "off−on" fluorescence signaling as guest binding results in either fluorescence quenching or inhibition of a quenching effect innate to the host.[23,24] Much less explored is the concept of a conformational switching process in which induced fit guest binding results in a marked change in host geometry that, in turn, influences signal intensity. We have applied this concept in the case of electrochemical sensors via a series of bis- and tris(ferrocenyl) podands.[1,2,25] As part of a versatile "modular" approach to di- and tripodal pyridinium derivatives capable of selectively binding and sensing anions using both organic[1,2] and inorganic[25] core moieties, we now describe the full characterization and remarkable dynamic and photochemical behavior of a simple, but highly effective, series of tripodal aminopyridinium-derived anion-binding hosts.

Results and Discussion

By adopting a modular approach to the preparation of anion host compounds, we have been able to prepare a versatile range of tripodal materials based on aminopyridines. Thus, reaction of 2-, 3-, or 4-aminopyridine with tri(bromomethyl)triethylbenzene **1**[13] results in the high-yield synthesis of compounds **2a**−**c** as bromide salts. Anion metathesis cleanly converts the compounds to the hexafluorophosphate analogues, Scheme 1. As a control, the analogous tris(pyridinium) species **3** and **4** were also prepared in a similar manner from **1** or tri(bromomethyl)-benzene, respectively. Functionalized derivatives were prepared via a procedure similar to that reported by us for the synthesis of the tris(ferrocenyl) compound **5**.[1] Thus, condensation of 3-aminopyridine with ethanal, benzaldehyde, 4-pentylbenzaldehyde, and anthracene-9-carbaldehyde gave imines **6**−**9**. These compounds were reduced to the corresponding amines **10**−**13** by treatment with borohydride. Reaction of **11**, **12**, and **13** with **1** followed by anion metathesis gave substituted hosts **15**, **16**, and **17** in unoptimized overall yields of 62%, 72%, and 51%, Scheme 2. The (*N*-ethylamino)pyridinium host **14** was isolated as the bromide salt, but counterion metathesis did not proceed cleanly and the compound was not explored further. The analogous 2- and 4-pyridyl isomers of **9**−**11** could be prepared, but clean analogues of **12**−**14** could not be isolated. For comparison, the bis(anthracenyl) molecular clips **18a**−**c** and the single-arm *N*-benzyl model compound **19** were also prepared, in good yield.

X-ray Crystallography. Compounds **3**, **2b**, and **2c** were all characterized by X-ray crystallography as bromide salts, and the hosts along with their immediate environments are shown in Figures 1−3, respectively. The model compound **3**, which does not contain a strong hydrogen bond acid group (i.e., an amine), exists as two pseudopolymorphs depending on crystallization conditions. The host species in these two forms of **3** exhibit radically different conformations with the orthorhombic **3**·3Br·EtOH (from ethanol/hexane) displaying a cone conformation with all three pyridinium arms orientated in the same direction (3-up or "3u", Figure 1a), while the triclinic **3**·3Br·4.5MeOH (from methanol/triethylamine) exhibits two crystallographically independent molecules both in the "2u, 1d" form (d = down). The orthorhombic form is able to incorporate a bromide anion within the molecular cavity formed by the three pyridinium groups. Crystal packing effects (formation of an edge to face $\pi-\pi$ interaction) also result in two methyl groups being orientated in the same way as the pyridinium groups despite the preference for alternation about the hexasubstituted core. The host interacts with the bromide anion via a six-fold array of pyridinium charge-assisted CH···Br^- hydrogen bonds with C···Br distances in the range 3.42−3.70 Å. Related CH···halide interactions have been shown to be important in pyridinium-[2] and imidazolium-based[26] hosts recently, and a growing weight of evidence suggests that they play an integral role in the present complexes (vide infra). The host adopts a T-shaped conformation rather than a symmetric C_3 geometry. This conformation allows the close approach to the bromide anion of an additional CH group from an adjacent host molecule. The coordination sphere of the intracavity bromide anion is completed by a hydrogen bond from enclathrated ethanol.

The "2u, 1d" conformation of the triclinic form is surprising and suggests that electrostatic interactions between pyridinium rings destabilize the usual 3u conformation in comparison to related systems,[4,5,15] in the absence of specific anion conformational templating. One of the two independent molecules in the structure binds bromide via CH···Br^- interactions between two pyridinium rings in a fashion comparable to the orthorhombic analogue (Figure 1b). The second independent molecule, however, binds methanol in a similar position and does not exhibit a specific anion-binding pocket. The structures imply that in the absence of strong hydrogen bonding functionality there is a fine balance between a variety of conformations and anion-binding modes. In the solid state, the host molecules in the triclinic form are arranged in offset dimers, linked by pairs of bromide anions binding to two pyridinium rings from one host and one from another, Figure 1b.

(23) Gawley, R. E.; Zhang, Q.; Higgs, P. I.; Wang, S.; Leblane, R. M. *Tetrahedron Lett.* **1999**, *40*, 5461−5465.
(24) Gunnlaugsson, T.; Davies, A. P.; Glynn, M. *Chem. Commun.* **2001**, 2556−2775.
(25) Wallace, K. J.; Daari, R.; Belcher, W. J.; Abouderbala, L. O.; Boutelle, M. G.; Steed, J. W. *J. Organomet. Chem.* **2003**, *666*, 63−74.
(26) Ihm, H.; Yun, S.; Kim, H. G.; Kim, J. K.; Kim, K. S. *Org. Lett.* **2002**, *4*, 2897−2900.

Scheme 2. Synthesis of Substituted 3-Aminopyridinium-Based Hosts

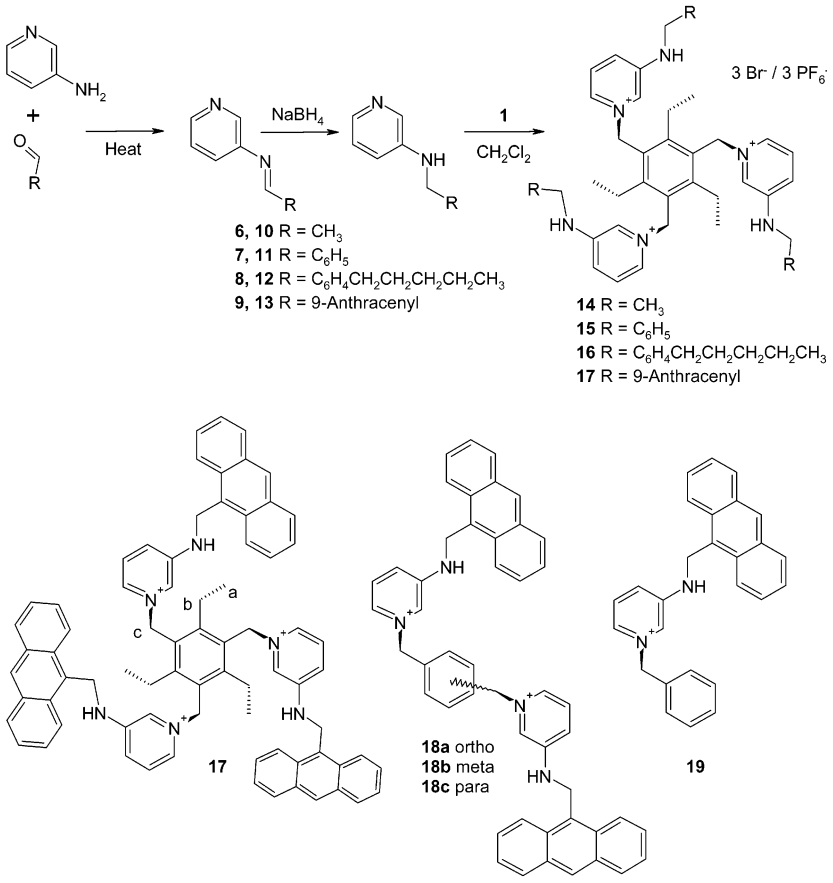

The bromide salt of compound **2b** was also found to exist in two pseudopolymorphic forms in the solid state, differing in the nature of the included solvent, although the conformation of the host and the anion-binding mode are very similar in both structures. The X-ray crystal structure of the monoclinic dichloromethane solvate of **2b**·3Br$^-$ (Figure 2) shows a remarkable encapsulation of an intracavity bromide anion by a six-fold array of NH···Br$^-$ and CH···Br$^-$ interactions. Two of the three NH groups are involved in interactions to bromide, which appears to be just slightly too large for the cavity (N···Br distances 3.35 and 3.40 Å). The remaining NH protons all interact with lattice bromide anions. The fact that not all three NH_2 groups interact with the intracavity Br$^-$ anion is thought to arise from the presence of three Br$^-$ anions in the structure and their effect on crystal packing. NMR and molecular modeling results on this and comparable systems[2] suggest that the solution structure, particularly in the presence of less than 3 equiv of halide, is dominated by the C_3 symmetric form (vide infra). The CH···Br$^-$ interactions with *ortho*-pyridyl CH groups C(6) and C(18) are longer than those in **3**, consistent with the dominance of the NH···Br hydrogen bonds. The bond to the hydrogen atom of the *ortho*-pyridyl CH group of the aminopyridinium arm that has its NH_2 group orientated away from the intracavity Br$^-$, C(8), is shorter and similar to those involved in **3**.

The X-ray crystal structure of the orthorhombic methanol solvate of **2b**·3Br$^-$ is essentially identical to the monoclinic form except that it involves a two-fold disorder of the one aminopyridinium ring that does not engage in NH···Br$^-$ interactions with the intracavity anion. This disorder is apparently linked to disorder of the lattice methanol solvent, and in both orientations the "arm" is able to maintain CH···Br$^-$ interactions as in the previous examples. It is noteworthy that the arms that chelate the intracavity anion via NH···Br$^-$ interactions are not subject to disorder.

Overall, it is clear from both structures that the host is highly complementary to bromide and to smaller halides, in general, and binds via multiple interactions in a chelating manner. This is in marked contrast to the structure of the analogous 4-aminopyridine derivative **2c** (Figure 3).

The 4-aminopyridinium derivative **2c**·3Br$^-$ adopts a partial cone conformation that is radically different from that observed for **2b** with a molecular cavity defined by two essentially coplanar pyridinium groups (reminiscent of two of the pyridinium rings in **3**) and two methyl substituents. The third pyridinium group is on the opposite face of the molecule. The molecular cavity is occupied by a molecule of methanol solvent which hydrogen bonds to a bromide anion sandwiched on the edge of the cavity between the coplanar pyridinium rings and held in place entirely by CH···Br$^-$ interactions. This very different structure for **2c** as compared to **2b** highlights the importance of the anion chelation in the case of the 3-aminopyridine derivative.

For comparison, host **2b** was also structurally characterized as the hexafluorophosphate salt (Figure 4). In the presence of PF_6^-, host **2b** adopts a "2u, 1d" conformation in stark contrast to the analogous bromide and is more reminiscent of **2c**·3Br. Unlike the structure of **2c** shown in Figure 3, however, Figure 4 reveals that **2b**·3PF_6 possesses two partial cavities, each of which includes a PF_6^- anion. Each anion interacts with one NH

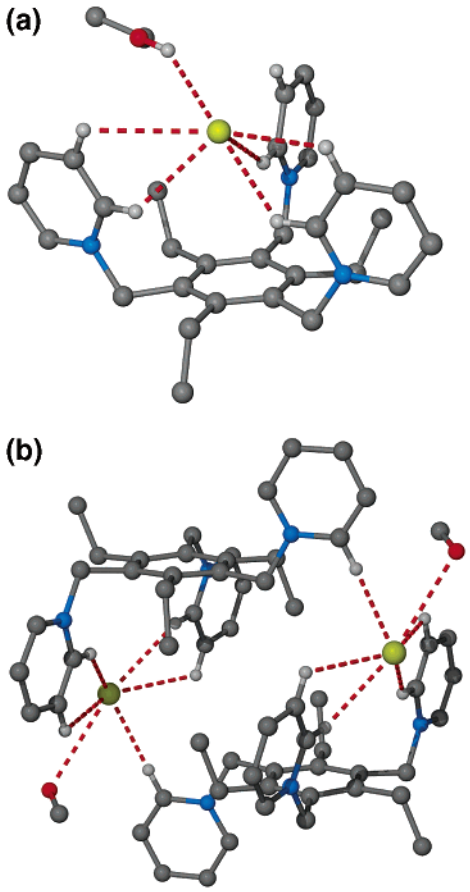

Figure 1. X-ray crystal structure of the model tris(pyridinium) species (a) **3**·Br_3·EtOH, (b) **3**·Br_3·4.5MeOH.

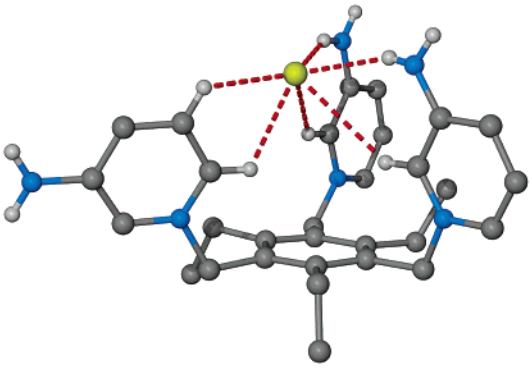

Figure 2. X-ray crystal structure of the tris(3-aminopyridinium) species **2b** as the bromide salt showing the chelation of a bromide anion by two of the three amino groups, supported by CH···Br^- interactions. In solution, a symmetric "3u, 3i" conformation predominates at low temperature.

functionality of a particular host. The anion also forms a number of additional intra- and intermolecular CH···F interactions.

The striking contrast of the nearly symmetrical chelate structure of **2b**·3Br^- as compared to **2b**·3PF_6^- and the partial cone (2u, 1d) **2c** clearly indicates a great deal of structural complementarity between **2b** and halide anions.

The anthracenyl receptor **17** was characterized by X-ray crystallography as the PF_6^- salt. The structure of **17**·3PF_6·MeOH·2MeCN shows that the cationic host adopts the 3u cone conformation expected for the hexasubstituted core[15] with alternation about the central arene ring. The NH groups and

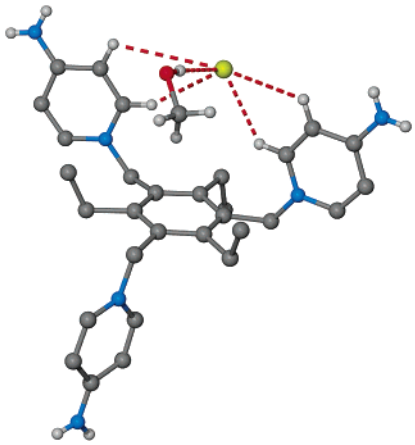

Figure 3. X-ray crystal structure of the tris(4-aminopyridinium) species **2c**. The host adopts a partial cone conformation. The host conformation dominated by the crystal packing which maximizes NH···Br^- interactions to the remaining anions.

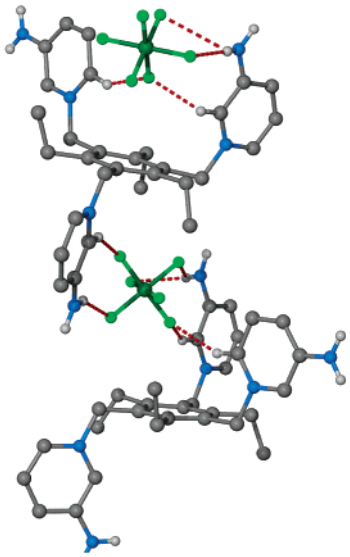

Figure 4. X-ray crystal structure of the tris(3-aminopyridinium) species **2b** as the hexafluorophosphate salt showing the two intracavity anion environments.

anthracene arms are splayed out, Figure 5, and do not converge on a central binding cavity.

We have termed conformations involving an NH group on the outside of the central cavity as "out" or "o"; hence the present system may be described as "3u, 3o" and contrasts to the bromide salt of the unsubstituted tris(3-aminopyridinium) receptor **2b**·3Br which adopts a "3u, 2i, 1o" conformation in both pseudopolymorphs (i = "in"), Scheme 3b. It is characteristic of "out" pyridinium rings that they engage in CH···anion interactions. In this case, there is a single PF_6^- anion which sits in the central part of the cavity and interacts with the pyridinium groups by an array of CH···F interactions. Two of the NH groups interact with the other two PF_6^- anions, while the final NH functionality interacts with the only methanol molecule enclathrated in the crystal structure. This difference makes the receptor unsymmetrical. The fact that only two of the NH groups are binding to two of the PF_6^- anions and the third is found in the cavity is rather interesting. It suggests that the CH···F hydrogen bonds, together with the electrostatic

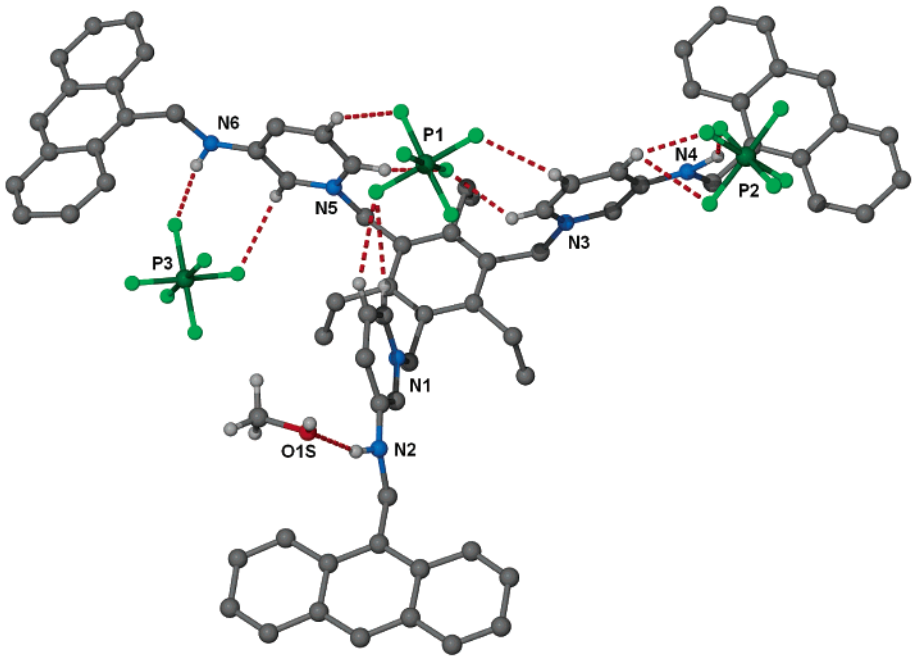

Figure 5. X-ray structure of receptor **17**·MeOH·2MeCN showing cooperative anion binding of the central PF_6^- anion by weak hydrogen bonds (hydrogen atoms removed for clarity). Selected hydrogen bond lengths, N(6)···F(16) 2.964(10), N(2)···O(1S) 2.926(10), N(4)···F(11) 3.239(14), C···F 3.022(15)−3.417(15) Å.

Scheme 3. Conformational Equilibria in 3-Aminopyridinium-Based Hosts (a) "3u" and "2u, 1d" Exchange, (b) In−Out Exchange (X = H, CH_2Ph, $CH_2C_6H_4(CH_2)_4CH_3$)

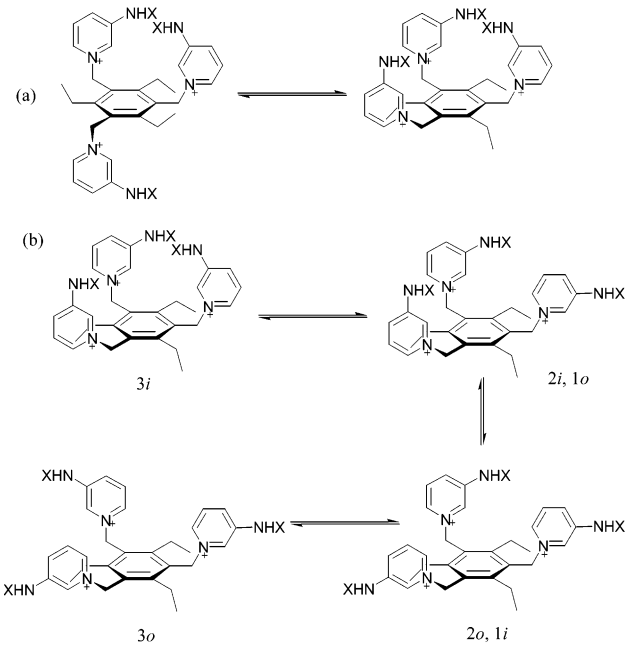

interactions, are more significant than the NH···F interaction alone, and hence the PF_6^- anion is found sitting in the central anion-binding pocket of the host, despite the lack of strong hydrogen bonds.

Grepioni and Braga have shown that in the solid state different organometallic compounds containing PF_6^- as the counterion form C−H···F−P hydrogen bonding interactions[27] that play a significant role when assisted by the difference in charge between the anions and the cation. In contrast, Howard and O'Hagan have also conducted a database search (up to 1996) to investigate the importance of fluorine as a hydrogen bond acceptor when the fluorine is covalently connected to carbon.[28,29] They found that there are few examples of C−F···H−X contacts that are below 2.35 Å. This conclusion is also supported by work carried out by Dunitz and Taylor who have carried out database analysis and theoretical calculations that show that contacts of type C−F···H−X (X = O, N, and C) do not form hydrogen bonds.[30] The cutoff distance for a C−H···F interaction is greater than 2.6 Å (the van der Waals radius), but there are many examples in which the hydrogen bonding distance is below the van der Waals radius. Grepioni and Braga have also shown that most of the shortest distances for C−H···F−P interactions are found when there is a metal coordinated to either cyclopentadienyl or arene ligands. Dunitz and Taylor also confirmed that when fluorine is part of an anion, for example, PF_6^-, the fluorine becomes a rather good hydrogen acceptor.[30]

Receptor **17** contains three PF_6^- anions. The anion in the middle of the cavity is bonded by five CH···F interactions with the distances ranging from 2.34 to 2.66 Å (CH bond length normalized to 0.96 Å) in good agreement with the distances obtained by Grepioni and Braga.[27] The two other PF_6^- ions are hydrogen bonding to the NH groups with hydrogen bonding distances of 2.11 and 2.26 Å, which represent relatively strong hydrogen bonds for these types of interactions.

NMR Titrations. The anion-binding ability of hosts of type **2** and compounds **3**, **4**, and **15**−**17** was investigated by ^{1}H NMR titration at room temperature in MeCN-d_3. The binding constants for the first anion derived from a model incorporating a final host:guest stoichiometry of 1:3 are summarized in

(27) Grepioni, F.; Cojazzi, G.; Draper, S. M.; Scully, N.; Braga, D. *Organometallics* **1998**, *17*, 296.

(28) Howard, J. A. K.; Hoy, V. J.; O'Hagan, D.; Smith, G. T. *Tetrahedron* **1996**, *52*, 12613.

(29) Borwick, S. J.; Howard, J. A. K.; Lehmann, C. W.; O'Hagan, D. *Acta Crystallogr., Sect. C* **1997**, *53*, 124.

(30) Dunitz, J. D.; Taylor, R. *Chem.-Eur. J.* **1997**, *3*, 89−98.

Table 1. Binding Constants (K_1) Determined by ^{1}H NMR Titration for the Interaction of the New Hosts with Various Anions[a]

	host K_{11} (M^{-1})						
anion	**2b**	**3**	**4**	**15**	**16**	**17**	**5**[2]
Cl^-	>100 000			>100 000	6452	5270	17 380
Br^-	13 800	850	17	3953	2330	486	2950
I^-				675	198	355	1860
NO_3^-	467			200	246	617	1410
$CH_3CO_3^-$	10 500			2511	1389	49 000	3680
ReO_4^-				112		4	4
$CF_3SO_3^-$				7			

[a] Anions as *n*-Bu_4N^+ salts in MeCN-d_3, host NH, *ortho*-pyridyl protons, and CH_2 groups fit simultaneously with HypNMR 2000.[32,53] Errors in K_1 are <10%. In some cases, precipitation occurred during the latter parts of the titration, and data so affected were discarded. Equilibria were modeled according to the binding of up to three anions by each host. Binding of the second and third anions was generally found to be weaker than the first, although it was nonnegligible and in the region of 10−100 M^{-1}.

Table 1. Data for the previously reported **5** are included for comparison.[2] The analysis was carried out with the aid of HypNMR 2000.[31,32] The unsubstituted tris(pyridinium) species **3** gives K_{11} = 850 M^{-1} for Br^- which represents the effect of cooperative electrostatic and CH···Br^- interactions. Removal of the preorganization imparted by the three ethyl functionalities (host **4**) reduced the binding to 17 M^{-1}, corresponding to a preorganization contribution of ca. 10 kJ mol^{-1} for **3** and implying a significant degree of cooperativity between the three arms in binding the first anion. The fact that a significant interaction is found between **3** and Br^- is interesting evidence in support of the importance of CH···Br^- interactions, particularly because this affinity essentially disappears upon examination of the nonethyl control compound **4**.

Host **2b** proved to be an extremely effective anion receptor with an affinity for Cl^- too high to measure in the chosen medium (K_{11} > 100 000 M^{-1}). The Br^- anion was also bound strongly, as was the highly basic acetate. Significantly, halides such as Br^- are much more strongly bound by **2b** than by **3**, consistent with the involvement of the more acidic NH functionalities and confirming the implications from the X-ray crystal structures of **2b** and **3** that NH···Br^- interactions are stronger than the analogous pyridinium CH···Br^- hydrogen bonds. The position of the NH group in **2b** is also more complementary to Br^- binding than the *meta*-pyridinium CH in **3**. It is also clear evidence for structural selectivity that Cl^- and even Br^- are bound more strongly than acetate. Acetate is a highly basic anion that can form a two-point interaction with NH and CH groups on a single "arm" or with two NH groups on adjacent arms, and hence it would be expected to form intrinsically more stable complexes with the aminopyridinium functionalities of hosts of type **2b**. However, the acetate complex cannot adopt a tris(chelate) C_3 symmetric conformation simultaneously maximizing interactions to all three arms. Similarly, host **2b** is also clearly sterically noncomplementary to NO_3^- (which is also intrinsically less basic than acetate) and hence is weakly bound.

At room temperature, all spectra display C_3 symmetry in contrast to the X-ray crystal structure of **2b**·$3Br^-$. The largest chemical shift changes ($\Delta\delta$) on addition of Cl^- are noted for the NH protons and pyridinium ortho CH singlet signal, and it is these protons that interact most with the anion in the solid state.

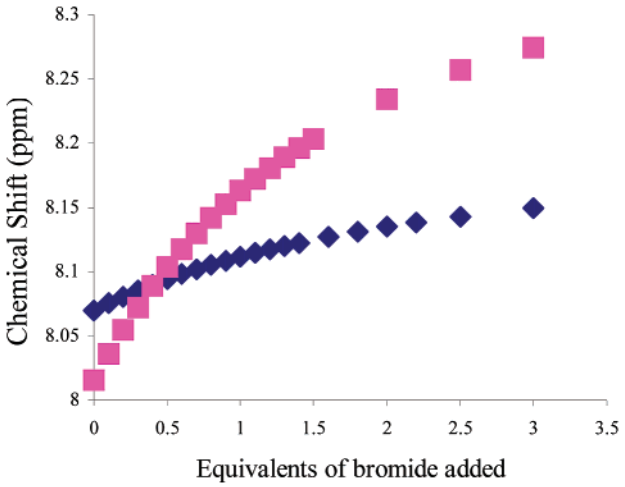

Figure 6. Chemical shift of the *ortho*-pyridyl CH resonance of **2b** (pink square) and **2c** (blue diamond) on the addition of NBu_4Br in DMSO-d_6 at 297 K.

Attempts were made to compare the anion-binding ability of **2b** with its isomers **2a** and **2c**. Unfortunately, in acetonitrile, addition of small quantities of halide anions to both **2a** and **2c** caused immediate precipitation. In contrast, in DMSO-d_6, only very weak binding of Cl^- was observed for both **2b** and **2c** (K_{11} = 15 and 8 M^{-1}, respectively), consistent with the highly competitive nature of the solvent and relatively nonacidic nature of the primary amine donors when compared to amides or ureas, for example.[21,33,34] In a mixture of DMSO/acetonitrile (50% v/v), **2b**·$3PF_6^-$ bound chloride extremely strongly (K_{11} = ca. 82 000 M^{-1}). The analogous figure for **2c**·$3PF_6^-$ in the DMSO/acetonitrile solvent mixture was ca. 3000 M^{-1}, although solubility constraints rendered this measurement rather imprecise. The greater effect upon addition of anions to **2b** as compared to **2c** in DMSO-d_6 is highlighted by the titration plots, however, Figure 6.

The substituted 3-aminopyridine hosts **15** and **16** showed behavior similar to that of **2b**, although the presence of the bulky benzyl groups results in a reduction of the affinity for halide anions. This inhibition is attributed to unfavorable steric interactions between the N-substituents when folded into the C_3 symmetric "3-up, 3-in" ("3u, 3i") conformation that is necessary to bind spherical anions (Scheme 3). These steric interactions could potentially contribute to the observation of alternative conformers despite the alternation preference of the hexasubstituted core, and the involvement of non-C_3 conformers in binding nonspherical anions such as PF_6^- is clearly indicated by variable-temperature ^{1}H NMR spectroscopy (vide infra). Examination of the shape of the titration curves shows that nonspherical anions are bound very differently to halides. Thus, in the case of Br^- binding by the tris(benzyl) host **15**, the titration curve for both NH and singlet pyridyl CH protons essentially reaches saturation at a host:anion ratio of 1:1. On titrating **15** with acetate, however, clear evidence is observed of significant interactions of both the NH and the *ortho*-pyridyl CH protons with a second anion in a fashion consistent with

(31) Frassineti, C.; Ghelli, S.; Gans, P.; Sabatini, A.; Moruzzi, M. S.; Vacca, A. *Anal. Biochem.* **1995**, *231*, 374−382.
(32) Gans, P. HypNMR 2000, University of Leeds: Leeds, 2000.
(33) Beer, P. D.; Cadman, J. *Coord. Chem. Rev.* **2000**, *205*, 131−155.
(34) Berrocal, M. J.; Cruz, A.; Badr, I. H. A.; Bachas, L. G. *Anal. Chem.* **2000**, *72*, 5295−5299.

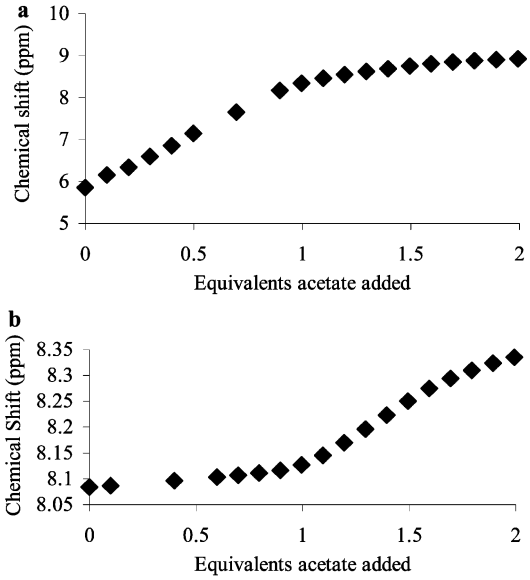

Figure 7. ^{1}H NMR titration plot of compound **17** and NBu_4MeCO_2 at room temperature in MeCN-d_6 (a) following the NH proton and (b) the pyridinium singlet, H(s). Some points are missing due to overlap of resonances.

that of nonconvergent binding sites. This effect becomes extremely pronounced in the very bulky tris(anthracenyl) analogue **17**.

Compound **17** is able to bind halide anions in the order $Cl^- > Br^- > I^-$; however, the affinity for halides is greatly reduced (by at least an order of magnitude), even more than for **5**, **15**, and **16**. Because the most effective halide binding occurs via a C_3 symmetric "3u, 3i" conformation in which the halide is chelated by all three NH groups, halide affinity is lowered as a consequence of unfavorable steric interactions between the bulky anthracenyl arms in this convergent geometry. This destabilization of the "3u, 3i" geometry remarkably increases the affinity of **17** for the less symmetric acetate anion, and indeed **17** is highly acetate selective with a binding constant almost too high to measure by NMR (49 000 M^{-1}), comparable to that recently observed by Beer et al. for a rigidly preorganized calixarene-based host system.[35] The acetate anion also remarkably gives a large chemical shift change, attributed to its strong binding and high basicity ($\Delta\delta$ 3.07 ppm for the NH protons in **17**). Close examination of the behavior of various nuclei as a function of added anion suggests that acetate binding by **17** occurs in a way different from the binding of halides. The very gradual change in the chemical shift behavior of the pyridyl singlet resonance, H(s), on addition of acetate is in marked contrast to the near saturation of the chemical shift change in this resonance after the addition of 1 equiv of halide anion (Figure 7) and suggests that this hydrogen atom is not directly involved in binding the first acetate anion. Addition of more than 1 equiv of acetate results in more significant changes to this resonance. These observations could be interpreted as binding of the first acetate anion in a chelating fashion by two NH moieties from adjacent arms and binding of the second to the NH and CH moieties of the remaining arm, Figure 8. This binding mode may just as readily occur in both "3u, 2i, 1o" and "3u, 1i, 2o" conformers in which the anthracene units are not forced into

(35) Beer, P. D.; Drew, M. G. B.; Hesek, D.; Nam, K. C. *Organometallics* **1999**, *18*, 3933.

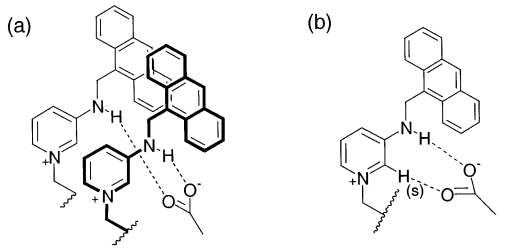

Figure 8. Proposed binding modes between receptor **17** and $MeCO_2^-$ (a) first anion via NH···O interactions and (b) second anion via NH···O and CH(s)···O interactions.

Table 2. The Maximum Chemical Shift Changes (ppm) Observed on the Addition of 0.7 equiv of NBu_4X, Added to the Molecular Clips **18a**−**c**

	Δδ/ppm					
	Br^-		NO_3^-		$MeCO_2^-$	
compound	NH	PyH	NH	PyH	NH	PyH
18a	0.23	0.25	0.19	0.11	2.00	0.31
18b	0.12	0.13	0.22	0.08	2.28	0.66
18c	0.15	0.11	0.26	0.10	1.90	0.23

close mutual proximity. This proposal is supported by variable-temperature NMR studies (vide infra), which show evidence for acetate complexation by up to four conformers. In hosts where steric interactions are less important, the acetate-selective out conformations are less prevalent, consistent with the variable-temperature NMR results for **2b**. Also, a low binding constant is obtained on titrating acetate with the model compound **19**, for which the binding affinity was calculated to be 7 M^{-1}. Hence, the highly sterically hindered nature of receptor **17** may predispose it to adopt a series of conformations preorganized for chelate acetate binding at the expense of the halide selective "3u, 3i" geometry.

Unfortunately, accurate binding constants for the molecular clips **18a**−**c** could not be obtained for comparison due to solubility constraints. However, on the addition of 0.7 equiv of NBu_4X (X = Br, NO_3, and $MeCO_2$) to a solution of MeCN-d_3 containing the receptors, small shifts were observed for the NH protons and the ortho CH proton on the pyridinium ring. The largest chemical shift change seen for the NH proton was obtained for the meta isomer on the addition of acetate, Table 2. This result suggests that a chelate effect occurs more for the meta isomer than the ortho and para isomers, which is in good agreement to the analogous ferrocenyl dipodal hosts.[1]

Variable-Temperature ^{1}H NMR Spectroscopy. In the case of **2b**, addition of substoichiometric amounts of chloride in acetonitrile results in an immediate and dramatic broadening of the ^{1}H NMR spectrum, clearly indicative of a dynamic process occurring at a rate comparable to the ^{1}H NMR spectroscopic time scale. Because of the high freezing point of acetonitrile, the ^{1}H NMR spectrum of **2b** as a function of temperature (297−183 K) was examined in acetone-d_6 solution (a) as the hexafluorophosphate salt, (b) in the presence of 0.4 equiv of NBu_4Cl, and (c) in the presence of 0.8 equiv of NBu_4Cl (precipitation occurred after the addition of 1 equiv). The resulting spectra are shown in Figure 9. Before addition of chloride (Figure 9a), the spectrum is essentially constant down to 223 K at which temperature significant broadening occurs, with coalescence at 203 K. At 183 K, two sets of resonances are evident with splitting particularly noticeable for the signals

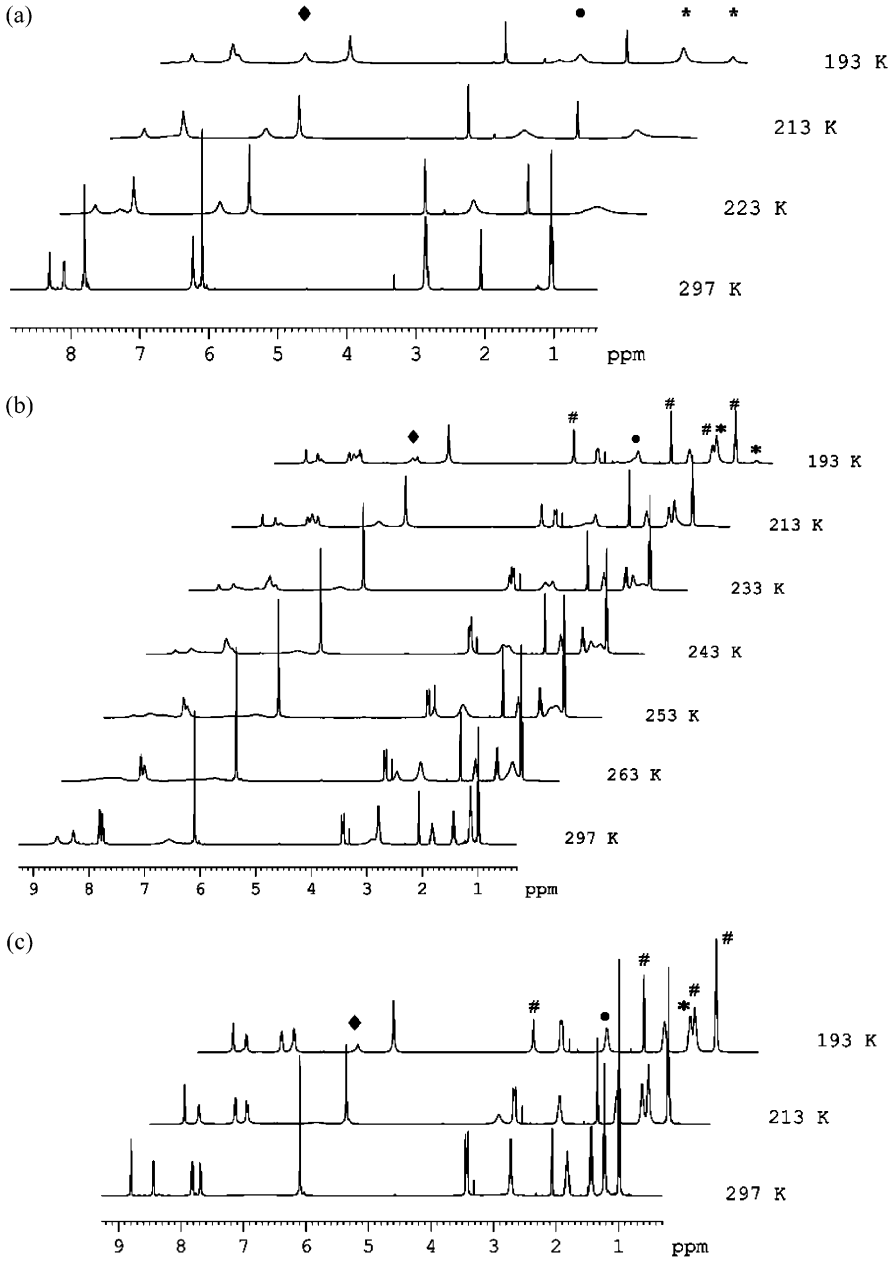

Figure 9. Variable-temperature ^{1}H NMR spectra of **2b** in acetone-d_6 (a) as the hexafluorophosphate salt, (b) after addition of 0.4 equiv of NBu_4Cl, and (c) after addition of 0.8 equiv of NBu_4Cl. # NBu_4Cl, ∗ ethyl CH_3 (Ha), ● ethyl CH_2 (Hb), and ◆ NH (Hc).

associated with the ethyl groups of the triethylbenzene-derived core. The CH_3 resonance of the ethyl groups at δ 1.03 ppm is characteristically split into two new signals in the ratio 4:1 at 1.32 and 0.55 ppm. The high field chemical shift of the latter signal is attributed to a host conformation in which the ethyl group enters the shielding region of one of the pyridinium rings. Such features are evident in all of the X-ray crystal structures discussed above, particularly Figure 1b, and it is likely that the fluxionality of **2b**·3PF_6 is associated with a conformational equilibrium of six substituents around the hexasubstituted aromatic core. This fluxionality could take the form of a minor conformational change involving rotation of the ethyl groups or a much more substantial rotation of the pyridinium substituents, Scheme 3a. Electrostatic arguments would tend to suggest that it arises from the mutual repulsion of the pyridinium cations to give a 2-up, 1-down isomer, and indeed the spectrum of the minor conformer is less symmetrical than the major species. This postulate is confirmed by the freezing out of additional minor conformers in more bulky systems (vide infra).

Addition of 0.4 equiv of NBu_4Cl to the sample and repeating the variable-temperature experiment reveals an addition fluxional process, that coalesces at much higher temperature, Figure 9b. Broadening is immediately noted in the room-temperature spectrum, with coalescence occurring at 253 K. Below this temperature, two sets of resonances in a ratio of 3:2 are observed down to 223 K at which point one set of resonances (the major set) undergoes further broadening along the pattern outlined above for **2b**·3PF_6. The other signals remain sharp down to 183 K. The slightly lower intensity of the sharp resonances as compared to those that broaden at 223 K allows us to unambiguously assign them to the chloride complex **2b**·Cl·2PF_6 which is conformationally rigid on the ^{1}H NMR time scale, C_3 symmetric, and coexists with the remaining **2b**·3PF_6 responsible for the major set.

In a final VT experiment, a total of 0.8 equiv of Cl^- was added to host **2b**. This experiment showed a spectrum that remained essentially constant down to 183 K with some broadening as a result of the residual **2b**·$3PF_6$ and solvent viscosity effects. Differentiation of the NH signal into two resonances was also observed, consistent with the preferential interaction of the Cl^- anion with the NH proton pointing into the cavity. Thus, the second, high-temperature fluxional process is attributed to the freezing of the anion exchange equilibrium between **2b**·Cl·$2PF_6$ and **2b**·$3PF_6$. This is extremely unusual in podand anion-binding hosts, which generally display fast anion exchange kinetics.[36−39] We note, however, that slow exchange of NMe_4Cl has recently been reported by Atwood and Szumna for an elegant resorcarene-based tetrapodal molecular capsule.[40] Even more remarkably, the fact that **2b**·Cl·$2PF_6$ is conformationally rigid and exhibits, for example, only a single peak for the terminal CH_3- group of the ethyl moieties at all temperatures, and is C_3 symmetric, clearly indicates that binding of Cl^- is by a C_3 symmetric "3u, 3i" conformation and that conformation is stabilized as compared to the "2u, 1d" partial cone conformer observed for the PF_6^- salt (cf., Figure 4 and Scheme 3a). Moreover, the unhindered nature of **2b** results in essentially all of the sample being present as a 3i isomer (Scheme 3b) in contrast to the X-ray structure of **2b**·$3Br^-$ (Figure 2). Thus, **2b**·$3PF_6$ exists as an equilibrium mixture of cone and partial cone conformers; **2b**·Cl·$2PF_6$ is purely a cone isomer consistent with the strong binding observed by NMR titration. This observation represents a nice example of induced fit binding in an entirely artificial, anion-binding system. The strong binding of chloride by **2b** and slow exchange kinetics may be explained by the encapsulation of the anion in a highly complementary trigonal prismatic array of hydrogen bonds from both NH and pyridinium CH moieties of the host, broadly consistent with Figure 2 and modeling studies on related ferrocenyl derivatives.[2]

Given that the high field peak at 0.55 ppm observed in Figure 9a is absent in Figure 9c at 183 K, we can confidently assign it to a partial cone isomer of **2b**·$3PF_6$ which is likely to have two of the three methyl groups in the shielding region of the pyridinium rings, as demonstrated structurally in Figures 1a and 4. Integrating the two resonances in the low-temperature ^1H NMR spectrum allows the calculation of an equilibrium constant at 183 K for the two conformations of the PF_6^- salt of 2.0 M^{-1}, suggesting that the energy difference between them is minimal (ca. 1 kJ mol^{-1}). This is in contrast to values of 10−15 kJ mol^{-1} suggested for the stabilization of the "3-up" conformer by a hexasubstituted aromatic core in related systems[5] and probably arises from the destabilization of the "3-up" conformer by binding the bulky PF_6^-, as suggested by molecular modeling in the case of the tris(ferrocenyl) appended analogue.[2]

The variable-temperature ^1H NMR spectra of the bulky hosts **15** and **16** as the hexafluorophosphate salts display behavior essentially similar to that of **2b** except for two key differences: first, the unsymmetrical "2-up, 1-down" conformer is much more evident for the PF_6 salts (essentially 50% of the sample) consistent with the destabilizing of the C_3 "3-up" isomer by steric clashes between the aryl substituents. Second, a large number of signals are noted for the protons of the ethyl substituents consistent with the freezing out of a number of isomers arising from the in−out pyridinium rotation (Scheme 3a and 3b), not observed in the case of **2b** (we have observed fluxionality of 3-aminopyridyl derived ligands in related metal-based anion hosts[25]). For example, the single peak at 0.55 ppm assigned to the shielded methyl protons in the "2-up, 1-down" conformation in **2b** appears as four separate signals from 0.1 to 0.6 ppm in **15** and **16** at 183 K. Coalescence of the methyl signals is also observed at a slightly higher temperature in **15** and **16** (233 K, as compared to 223 K in **2b**).

Addition of 0.4 equiv of Cl^- to both **15** and **16** results in an extremely broad room-temperature spectrum, and the coalescence temperature for the CH_3 resonance is 283 K (cf., 253 K in **2b**). As in **2b**, moving to lower temperature results in the initial observation of two sets of resonances consistent with time-averaged C_3 symmetry for the chloride complex, but at 233 K one set of resonances, assigned to **15**·$3PF_6^-$ (or the **16** analogue), broadens and splits further. The other set assigned to **15**·Cl^-·$2PF_6^-$ or **16**·Cl^-·$2PF_6^-$ remains generally sharp and C_3 symmetric down to the solvent limit at 183 K, although other signals of low intensity are detected at very low temperature. In the presence of 0.8 equiv of Cl^-, the signals assigned to the hexafluorophosphate salt are markedly diminished in intensity, and the spectrum is almost temperature invariant. Additional resonances corresponding to ca. 10% of the sample are observed, however, and these are assigned to alternative 3u isomers with an out conformation of the pyridinium rings, as in Scheme 3b.

Similar VT ^1H NMR experiments on **2b** and **15** were repeated with Br^-, I^-, $CH_3CO_3^-$, and NO_3^-. For the bulky compound **15**, the spectra in each case remain invariant down to ca. 233 K, at which point a single equilibrium process apparently freezes out. While slow anion exchange as in the case of Cl^- cannot be ruled out, the spectra may be rationalized by a model involving fast anion exchange even at low temperature coupled with slow conformational exchange of the type shown in Scheme 3b. All of the anions apparently stabilize the "3-up" conformation relative to "2-up, 1-down"; however, the proportion of out conformers of **15** increases going down the halides and reaches almost 50% for I^-. Acetate, which is strongly bound, is also effective at stabilizing the "3u, 3i" conformer, and the complex has time-averaged C_3 symmetry, although the static symmetry must be lower. The more weakly bound NO_3^- is less effective, and even in the presence of 1.1 equiv of NO_3^- (no precipitation), a significant amount of out conformer is evident. For the less hindered **2b**, no evidence is observed for in and out conformers as a result of the absence of steric interactions disfavoring the 3i form.

In view of the interesting VT results obtained for **2b**, **15**, and **16**, the ^1H NMR spectrum of the previously reported[1,2,41] tris(ferrocenyl) compound **5** was also examined in the presence of 0.4 equiv of Cl^- at various temperatures. As with **15** and **16**, the room-temperature spectrum proved to be extremely broad, and at 283 K two sets of resonances could be discerned assigned to **5**·Cl·$2PF_6$ and **5**·$3PF_6$, respectively. Lowering the

(36) Renard, S. L.; Kilner, C. A.; Fisher, J.; Halcrow, M. A. *J. Chem. Soc., Dalton Trans.* **2002**, 4206−4212.
(37) Hettche, F.; Reiss, P.; Hoffmann, R. W. *Chem.-Eur. J.* **2002**, *8*, 4946−4956.
(38) Causey, C. P.; Allen, W. E. *J. Org. Chem.* **2002**, *67*, 5963−5968.
(39) Denuault, G.; Gale, P. A.; Hursthouse, M. B.; Light, M. E.; Warriner, C. N. *New J. Chem.* **2002**, *26*, 811−813.
(40) Atwood, J. L.; Szumna, A. *J. Am. Chem. Soc.* **2002**, *124*, 10646−10647.
(41) Zhang, J.; Bond, A. M.; Wallace, K. J.; Belcher, W. J.; Steed, J. W. *J. Phys. Chem. B* **2003**, *107*, 5777−5786.

temperature to 243 K resulted in the dramatic broadening of one set of resonances. At 183 K, a relatively sharp spectrum was observed which could be assigned to a static mixture of predominantly 3u, 3i-**5**·Cl·2PF_6 and a mixture of 3u and 2u, 1d conformers of **5**·3PF_6. Small amounts of out conformers were observed for both species consistent with the bulk of the ferrocenyl group.

As with the previous hosts, the ^{1}H NMR spectrum of **17** as a function of temperature (297−183 K) was examined in acetone-d_6 solution (a) as the hexafluorophosphate salt, (b) in the presence of 0.4 equiv of NBu_4Cl, and (c) in the presence of 0.8 equiv of NBu_4Cl (precipitation occurred after the addition of 1 equiv). The ^{1}H NMR spectrum for **17**·3PF_6 is sharp at room temperature. Cooling brings about an immediate broadening in the resonances associated with the pyridinium rings and ethyl substituents. Coalescence occurs at 233 K, and at 183 K the spectrum is relatively sharp. The resonance assigned to the CH_3 group of the ethyl substituents splits into two groups of three peaks (six in all) centered on 1.4 and 0.9 ppm. The presence of a high field signal under 1 ppm is indicative of a CH_3 group that is in the shielding region of one of the pyridinium rings and is a characteristic of a "2u, 1d" conformation (cf., **2b**). The intensity distribution suggests that, as for the unsubstituted 3-aminopyridinium analogue, an approximately 2:1 mixture of "3u" and "2u, 1d" conformations is present. In compounds such as **2b**, we only observe two peaks of this type. The fact that six are observed in this case suggests that additional conformational equilibria have been frozen out. Similarly, the resonance assigned to the CH_2 group bonded to the pyridinium nitrogen atom splits into four signals rather than the usual two. The remainder of the spectrum is likewise unsymmetrical, Figure 10. Interestingly, the protons assigned to the anthracene groups remain relatively sharp, suggesting that the anthracene moieties are conformationally mobile and independent from the core. Hence, it is likely that the additional peaks are due to slow exchange between in and out conformers of the pyridinium rings.

On addition of substoichiometric amounts of chloride (0.4 equiv), there is immediate broadening of the ^{1}H NMR spectrum at 297 K, as observed for **5**, **15**, and **16**. Coalescence occurs at 273 K, and, for example, the peaks for the CH_2 groups bonded to the nitrogen on the pyridinium ring split into two distinct peaks in a 3:2 ratio as high as 253 K. This is consistent with the freezing out of the anion exchange equilibrium. On repeating the experiment on the addition of 0.8 equiv of Cl^-, the spectrum remains generally sharp to 263 K and then becomes broad. At low temperature (183 K), the spectrum is again unsymmetrical; however, unlike the low-temperature spectrum of **17**·3PF_3, the high field peaks between 0 and 1 ppm indicative of a "2u, 1d" conformation are absent, indicating that the host binds the anion in a "3u" cone conformation, probably of the "3u, 3i" type. The spectrum is consistent with the presence of one major isomer as indicated by a dominant pyridinium CH_2 signal at 6.07 ppm, along with a number of other minor conformers tentatively assigned to out isomers arising from rotation of the pyridinium rings.

The experiments with Cl^- were repeated with acetate, an anion lacking spherical symmetry and therefore likely to disfavor the C_3 symmetric "3u, 3i" conformation. The low-temperature spectra recorded in the presence of 0.4 equiv of anion show the coalescence of the anion exchange equilibrium at 243 K. In the presence of 0.8 equiv, an extremely unsymmetrical spectrum is observed at 183 K in stark contrast to **2b**, indicative of a number of conformers, although crucially none display the characteristic signals at ca. 0.9 ppm for the "2u, 1d" species. A total of four signals are observed which could be assigned to the acetate CH_3 group at −0.80, −0.91, −1.34, and −1.58 ppm, although they could also arise from highly shielded host ethyl groups. These signals are tentatively assigned to acetate binding by four isomers of the "3u" conformer arising from pyridinium group rotation, "3u, 3i", "3u, 2i, 1o", "3u, 1i, 2o", and "3u, 3o". The chemical shifts of these resonances indicate that the anions all fall within the shielding region of the anthracenyl or pyridinium rings.

UV−Vis Titration. The UV−vis spectra of receptors **15** and **16** as the hexafluorophosphate salts were measured in acetonitrile at a concentration of 2.5×10^{-5} M at room temperature. The spectra show a broad band at $\lambda_{max} = 348$ and 350 nm for **15** and **16**, respectively, assigned to the $\pi \rightarrow \pi^*$ transition of the pyridinium rings.[42] A strong band appears at approximately 200 nm, which is a characteristic band of benzene derivatives.[42]

On titration of **16** with NBu_4X (X = Cl, Br, I, and NO_3) from 0 to 10 equiv, there is a small but significant bathochromic shift of 3 nm in all cases, possibly indicative of a stronger hydrogen bond interaction between the anions studied in comparison to the poor hydrogen bond acceptor, PF_6^- anion. The observation of isosbestic points at $\lambda = 347$, 341, 331, and 341 nm for Cl^-, Br^-, I^-, and NO_3^-, respectively, means that there are only two species present under these conditions. For the three halides studied, the isosbestic point moves in the hypsochromic direction descending the series, an indication of the stability of the host−guest complex, which is becoming less stable going from chloride to iodide, in agreement with the ^{1}H NMR studies.

UV spectroscopy was also employed to provide further evidence for the conformational behavior of **17**. The UV spectrum of **17** shows two peaks at 248 and 255 nm assigned to a second electronic transition of the anthracenyl rings. Work carried out by Desvergne and Tucker has shown that the shape of the second electronic absorption band is related to the characteristic mutual interaction between two anthracene units.[43,44] In **17**, the band at 256 nm dominates in the free host situation. The overall intensity of the UV spectrum decreased on the addition of acetate, with an isosbestic point observed at 272 nm; however, the second electronic band at 248 nm increases somewhat in relative intensity, Figure 11b, indicating that the anthracene units are mutually interacting and that this interaction increases on the addition of acetate (cf., Figure 7). In contrast to these results, the UV spectrum of model **19** that only contains one anthracene moiety shows only a single band at 252 nm, assigned to the second electronic transition. There is a small shoulder that can be assigned to intermolecular interactions between two molecules of **19** in solution, whereas the band at 248 nm for **17** is due to the intramolecular interactions of the anthracene moieties. On addition of $MeCO_2^-$ to compound **19**,

(42) Lambert, J. B.; Shurvell, H. F.; Verbit, L.; Stout, G. H. *Organic Structural Analysis*; Macmillian Publishing: New York, 1976.
(43) Marquis, D.; Desvergne, J. P.; Bouaslaurent, H. *J. Org. Chem.* **1995**, *60*, 7984−7996.
(44) Tucker, J. H. R.; Bouas-Laurent, H.; Marsau, P.; Riley, S. W.; Desvergne, J.-P. *Chem. Commun.* **1997**, 1165−1166.

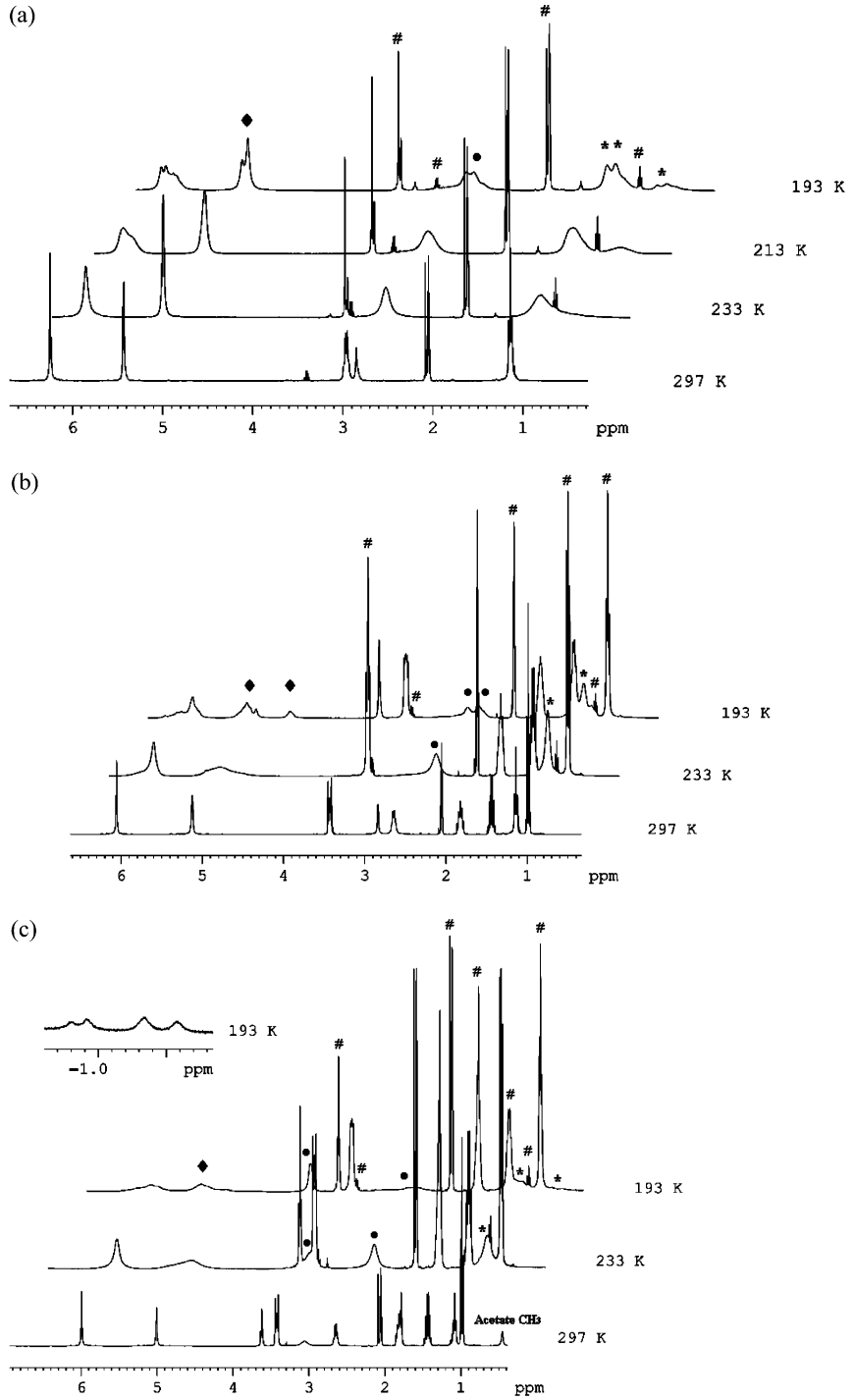

Figure 10. Partial variable-temperature ^{1}H NMR spectra in acetone-d_6 (a) as **17**·3PF$_6$, (b) **17**·3PF$_6$ plus 0.8 equiv of NBu$_4$Cl, and (c) **17**·3PF$_6$ plus 0.8 equiv of NBu$_4$MeCO$_2$. Note the splitting of the acetate methyl resonance at 0.45 ppm into four peaks between −0.7 and −1.8 ppm. # NBu$_4$X, and solvent peaks, ∗ ethyl CH$_3$ (Ha), ● ethyl CH$_2$ (Hb), and ◆ CH$_2$ (Hc) adjacent to the pyridinium nitrogen.

there is only a slight decrease in absorbance intensity, consistent with the weak binding observed by NMR. The experiment was repeated on the addition of NBu$_4$Cl to **19**. Again, only one band is observed at 254 nm. On the addition of Cl$^-$ to receptor **17**, the relative intensity of the band at 248 nm is unchanged, Figure 11a, and suggests that there is little change in the anthracene mutual interaction.

Fluorescence Studies. Compound **17** falls into the category of the fluorophore−spacer−receptor model proposed by de Silva,[18] and therefore the compound could act as a simple photoinduced electron-transfer (PET) sensor. However, the presence of more than one anthracene group, coupled with significant anion-dependent conformational changes on anion binding, suggests that additional effects may be observed arising from the anion-induced mutual interaction of anthracene moieties. An excited anthracene unit can associate with the ground state of a second fluorophore and produce an intramolecular excimer (anthracene−anthracene). Also, an excited-state anthracene−pyridinium complex (exciplex) could also be envisaged. The observation of such excimer or exciplex systems is

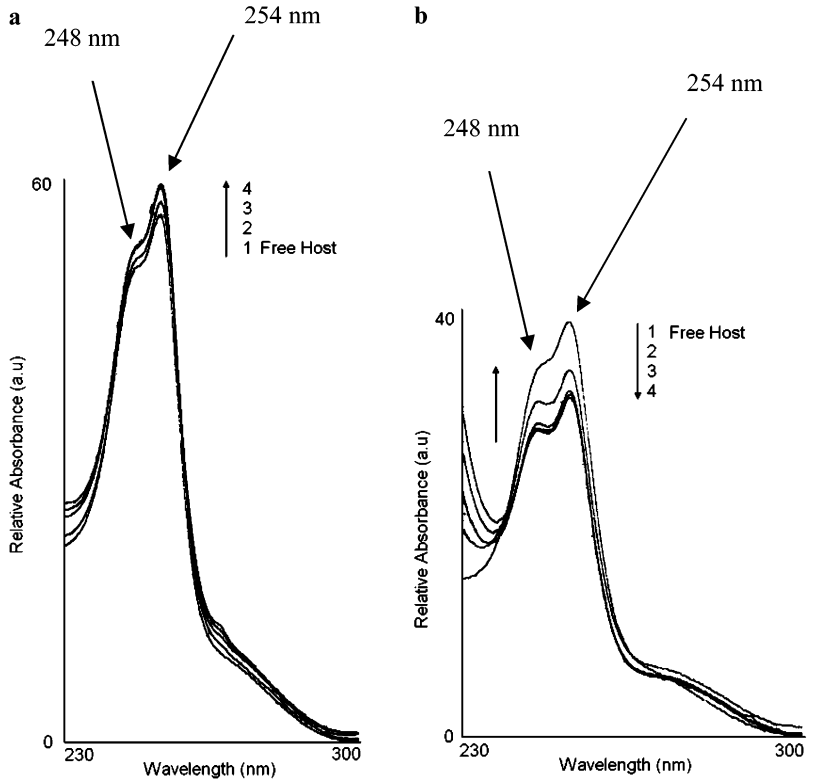

Figure 11. UV spectra of receptor **17** (1.0×10^{-6} M) on the addition of (a) NBu_4Cl and (b) NBu_4MeCO_2, at room temperature.

often dependent on the local concentration, which has been found to play an important role in fluorescence.[45,46]

A 1×10^{-5} M solution of receptor **17** was made up in a 2 cm^3 volume cell in MeCN and excited at 366 nm. The fluorescence emission spectrum was recorded straight away and displays monomer (single anthracene) emissions at 396, 416, and 440 nm. The fluorescence intensity of **17** was very low, approximately 100 (arbitrary units), when the sample was fresh; that is, fluorescence is quenched. However, it was observed that the fluorescence intensity increased when the solution was exposed to ambient light. Also, in some cases, the fluorescence spectrum of **17** showed evidence of the presence of an additional broad band at 540 nm possibly attributable to excimer or exciplex emission suggesting interaction of the arms with one another.

A simple experiment was carried out to see how much the fluorescence intensity increased over time. A fresh sample of receptor **17** and control **19** were subjected to UV irradiation (254 nm) over a 12 min period with spectra being recorded every 2 min. In both cases, the fluorescence intensity was observed to increase markedly, Figure 12. This result suggests that a more fluorescent species is being formed in solution. It is possible that this species is a result of $4\pi + 4\pi$ cycloaddition of two anthracene units. The fact that the fluorescence intensity of the control compound **19** is also increased implies that the cycloaddition between the anthracene moieties can occur in an intermolecular as well as an intramolecular fashion. Formation of addition products under UV irradiation is further supported by ^{1}H NMR spectroscopy. Exposure of an NMR sample of **17**

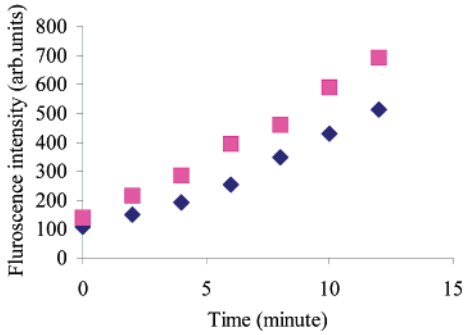

Figure 12. Plot of fluorescence intensity against time for **17**·$3PF_6$ (blue diamond) and **19**·PF_6 (pink square), irradiated at 254 nm at 2 min intervals.

to UV irradiation for 30 min resulted in the appearance of two small resonances at 4.51 and 4.52 ppm. The sample was run again after another 30 min, and the ^{1}H NMR spectrum was repeated and the intensities of these peaks became larger. Leaving the sample in the dark for 7 days and repeating the ^{1}H NMR measurement resulted in a reduction of the intensity of these signals, but they did not completely disappear, suggesting that the photoadduct is relatively long-lived. The appearance of two resonances in the NMR spectrum either can be assigned to cis and trans isomers of the photodimer or may represent the formation of both intra- and intermolecular addition species, particularly given the relatively high concentration of the sample in the NMR tube (20 mmol dm^{-3}). The appearance of one of the resonances is consistent with work carried out by Desverge and Tucker who designed an anthracene-derived receptor that can bind cations, in particular, sodium, in which the receptor can undergo a $4\pi + 4\pi$ cycloaddition reaction.[47] Evidence of this reaction has been obtained from UV spectroscopy and NMR

(45) Bouas-Laurent, H.; Casellan, A.; Desvergne, J.-P.; Lapouyade, R. *Chem. Soc. Rev.* **2000**, *29*, 43−55.
(46) Bouas-Laurent, H.; Castellan, A.; Desvergne, J.-P.; Lapouyade, R. *Chem. Soc. Rev.* **2001**, *30*, 248−263.

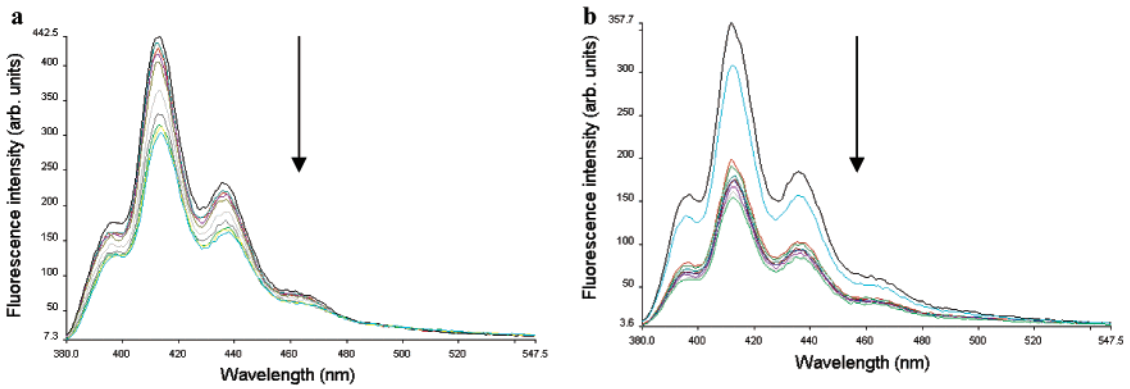

Figure 13. Fluorescence titration of receptor **17**·3PF_6 with (a) Cl^- and (b) I^- (MeCN, 2.5 × 10^{-5} M, addition of 20 equiv).

studies. In the ^{1}H NMR spectrum, the characteristic resonances of the tertiary bridgehead protons appear as a singlet at δ 4.56 ppm in $CHCl_3$,[48] in good agreement with our findings.

Titrations were carried out by adding 20 equiv aliquots of NBu_4X (X = Cl, Br, I, and $MeCO_2$) to a fresh sample of receptor **17**, but no significant change in fluorescence intensity was observed. If the sample was allowed to stand for an hour or so, however, the fluorescence intensity was observed to increase due to the formation of the cycloadduct. On addition of anions to these samples, the fluorescence intensity decreased in all cases; that is, quenching is observed. Emission is switched off by at least 30% on the addition of Cl^- and 50% for I^-, Figure 13.

Conclusions

A series of aminopyridinium-based receptors have been successfully synthesized in good yields. The binding ability of these hosts depends crucially on their ability to chelate the anion, and in the case of Cl^- extremely strong binding is observed along with slow anion exchange kinetics even at room temperature. Such strong non-Hoffmann selectivity is surprising in a host that operates via relatively poorly acidic NH···anion and CH···anion hydrogen bonding interactions.

The ethyl groups situated in the 2, 4, and 6 positions on the core introduce a degree of preorganization into the molecular scaffold forcing the pendant sidearms to point in the same direction as part of a "3-up, 3-down" or cone geometry; however, repulsions between the pyridinium rings destabilize this conformation in contrast to analogous neutral systems.[4−6,15] The 3-up conformer is further destabilized by unfavorable steric interactions in the case of compounds such as **15**−**17**, which have bulky substituents on the amino group. Anion binding results in a conformational switching process from 2-up, 1-down to 3-up that can be monitored by VT ^{1}H NMR spectroscopy.

Solubility problems have been encountered, which have rendered some of the binding constants imprecise. This problem was overcome by placing alkyl chains on the pendant sidearms in the successful synthesis of receptor **16**.

It has been shown by ^{1}H NMR titration and variable-temperature NMR work that receptor **17** is able to selectively bind acetate over spherical anions such as chloride. Acetate binding occurs via an equilibrating mixture of conformers with the first anion binding to a pair of pyridinium arms, resulting in an increase in the anthracene−anthracene mutual interaction. The high affinity for acetate is a result of the destabilization of the alternative 3-up, 3-in conformer that is more complementary to halides. The bulk of the anthracene units results in slow rotation of the pyridinium groups at low temperature. While receptor **17** is not an effective fluorescent sensor, it undergoes a 4π + 4π cycloaddition reaction to produce a more effective anion sensing species.

Experimental Section

General Considerations. Mass spectra were run at King's College London on a JEOL AX505W spectrometer in FAB mode in a thioglycerol or NBA matrix. NMR spectra were recorded on a Bruker AV-400 or AV-500 spectrometer operating at 400 or 500 MHz, respectively. IR spectra were recorded on a PE Paragon 100 FTIR spectrometer as Nujol mulls. Microanalyses were performed at London Metropolitan University. All reactions were carried out under nitrogen, although the products showed no oxygen or moisture sensitivity. The fluorescence spectra of the anthracene derivatives were made up in a concentration of 10 μM in MeCN. The NBu_4X salts were also dissolved in MeCN and added in aliquots of 10 μL to a 2.0 mL solution of the host, whereupon they were excited at 368 nm. The excitation wavelength was chosen from the absorption spectra. The spectra were recorded using a Perkin-Elmer luminescence spectrometer LS50B under PC control (FL Win Lab). UV/vis spectra were recorded in MeCN at ambient temperature using a Hewlett-Packard HP8453 diode-array spectrophotometer operating under a PC controlled using Hewlett-Packard software. The hosts were made up in 0.25 mmol solutions, and aliquots of NBu_4X salts were added to the 2.0 mL solution of the host in a cell of path length 1.0 cm.

NMR Titrations. A solution of the host (0.0500 M) was made up in a single NMR tube in the desired deuterated solvent (0.500 mL). Solutions of anions (0.2500 M) as the tetrabutylammonium salts were made up in a 2 mL volumetric flask, with the desired deuterated solvent. Ten microliter aliquots of the guest were added to the NMR tube with thorough mixing, and the spectra were recorded after each addition.

Materials. The preparation of **1** was carried out in accordance to the literature procedure.[13]

General Procedure for Counterion Metathesis. Method A: The relevant host bromide salt was dissolved in methanol (75 mL), and a methanolic solution of sodium hexafluorophosphate, in a 3-fold excess, was added to the bromide salt solution and left to stir at room temperature for 2 h. Over this time, the PF_6 salt precipitated. The solid was filtered, washed twice with methanol and then twice with diethyl ether, and dried in air for 24 h.

(47) McSkimming, G.; Tucker, J. H. R.; Bouas-Laurent, H.; Desvergne, J. P. *Angew. Chem., Int. Ed.* **2000**, *39*, 2167−2169.
(48) Wilson, D. T.; Selinger, B. K. *Photochem. Photobiol.* **1969**, *9*, 171.

Method B: The appropriate host bromide salt was dissolved in dichloromethane (75 mL), and an aqueous solution of sodium hexafluorophosphate (75 mL), in a 3-fold excess, was added to the bromide salt. The resulting biphasic solution was stirred for 2 h. The organic layer was separated, washed several times with water (100 mL), dried over magnesium sulfate, and filtered through Celite. The solvent was removed under reduced pressure, and the product was recrystallized as described below.

Syntheses. 1,3,5-Tris(2-aminopyridiniummethyl)-2,4,6-triethylbenzene Bromide (2a). 1,3,5-Tribromomethyl-2,4,6-triethylbenzene (1.00 g, 2.27 mmol) and 2-aminopyridine (0.640 g, 6.80 mmol) were dissolved in CH_2Cl_2 (50 mL) and stirred at reflux for 12 h. During this time, a white precipitate formed. This was filtered off and washed with CH_2Cl_2 (3 × 50 mL) to give the desired product as a white powder (0.87 g, 53%). ^{1}H NMR (400 MHz, MeOH-d_4, *J*/Hz, δ/ppm): 1.03 (t, $J = 7.4$, 9H, CH_3), 2.47 (q, $J = 7.4$, 6H, CH_2CH_3), 5.25 (s, 6H, $-CH_2-Py^+$), 6.82 (t, $J = 7.0$, 3H, PyH*p*), 7.15 (d, $J = 8.0$, 3H, PyH*m*), 7.31 (d, $J = 6.9$, 3H, PyH*o*), 7.81 (t, $J = 7.9$, 3H, PyH*m*). FAB-MS: *m*/*z* 641 $[M - Br]^+$. Anal. Calcd for $C_{30}H_{39}Br_3N_6$: C, 49.81; H, 5.43; N, 11.62. Found: C, 49.45; H, 5.88; N, 11.61.

1,3,5-Tris(3-aminopyridiniummethyl)-2,4,6-triethylbenzene Hexafluorophosphate (2b). 1,3,5-Tri(bromomethyl)-2,4,6-triethylbenzene (1.00 g, 2.3 mmol) and 3-aminopyridine (640 mg, 6.8 mmol) were refluxed for 6 h in chloroform (100 mL). The solvent was then removed under reduced pressure to produce the desired product as the tribromide salt (1.5 g, 1.3 mmol, 92%). ^{1}H NMR (MeOH-d_4, *J*/Hz, δ/ppm): 1.07 (t, 9H, $J = 7.5$, CH_3), 2.68 (q, 6H, 7.6, CH_2), 5.92 (s, 6H, CH_2), 7.6 (m, 3H, ArH), 7.73 (m, 3H, ArH), 8.26 (d, 3H, $J = 6.4$, ArH), 8.34 (s, 3H, ArH). FAB-MS: $m/z = 641$ $[M - Br]^+$, 561 $[M - 2Br]^+$. Anal. Calcd for $C_{30}H_{39}Br_3N_6$: C, 39.23; H, 4.28; N, 9.15. Found: C, 39.35; H, 4.02; N, 8.80. Counterion metathesis to give the hexafluorophosphate was achieved by method B described above. The solvent was removed under reduced pressure to produce the desired product, which was recrystallized from methanol and acetonitrile. Yield: 1.8 g, 2.0 mmol, 90%. ^{1}H NMR (MeCN-d_3, *J*/Hz, δ/ppm): 0.93 (t, 9H, $J = 7.5$ Hz, CH_3), 2.60 (q, 6H, 7.6, CH_2), 5.47 (s, br, 3H, NH) disappears on D_2O shake, 5.69 (s, 6H, CH_2), 7.64 (m, 6H, ArH), 7.65 (m, 3H, ArH), 7.81 (s, 3H, ArH). FAB-MS: $m/z = 774$ $[M - PF_6]^+$. IR (ν/cm^{-1}): 3508 *m*, 3412 *m* (NH_2), 837 *s* (PF_6 *br*). Anal. Calcd for $C_{30}H_{39}F_{18}N_6P_3 \cdot CH_2Cl_2$: C, 37.11; H, 3.92; N, 8.38. Found: C, 36.64; H, 4.05; N, 8.37.

1,3,5-Tris(4-aminopyridiniummethyl)-2,4,6-triethylbenzene Hexafluorophosphate (2c). 1,3,5-Tris(bromomethyl)-2,4,6-triethylbenzene (1.00 g, 2.3 mmol) and 4-aminopyridine (640 mg, 6.8 mmol) were refluxed for 6 h in chloroform (100 mL). The white precipitate that formed over this period was isolated by filtration and washed with CH_2Cl_2, to produce the desired product as a white solid. Yield: 1.5 g, 2.1 mmol, 91%. ^{1}H NMR (MeOH-d_4, *J*/Hz, δ/ppm): 0.87 (t, 9H, $J = 7.4$, CH_3), 2.62 (q, 6H, 7.4, CH_2), 5.50 (s, 6H, CH_2), 6.80 (d, 6H, $J = 7.3$, PyH), 7.80 (d, 6H, $J = 7.3$, PyH). FAB-MS: $m/z = 641$ $[M - Br]^+$. Anal. Calcd for $C_{30}H_{39}Br_3N_6 \cdot 4H_2O$: C, 40.43; H, 4.96; N, 11.82. Found: C, 41.06; H, 5.38; N, 12.16. Counterion metathesis to give the hexafluorophosphate was achieved by method A described above. Yield: 1.8 g, 1.9 mmol, 90%. ^{1}H NMR (DMSO-d_6, *J*/Hz, δ/ppm): 0.77 (t, 9H, $J = 7.2$, CH_3), 2.55 (q, 6H, $J = 1.0$, CH_2), 5.47 (s, 6H, CH_2), 6.85, 8.03 (AA′ BB′, 12H, $J = 7.3$, ArH), 8.15 (br, s, 6H, NH) disappears on D_2O shake. FAB-MS: $m/z = 774$ $[M - PF_6]^+$, 628 $[M - 2PF_6]^+$. IR (ν/cm^{-1}): 3443 *m*, 3311 *m*, 3204 *m* (NH_2); 842 *s*, *br* (PF_6). Anal. Calcd for $C_{30}H_{39}F_{18}N_6P_3$: C, 39.23; H, 4.28; N, 9.15. Found: C, 39.14; H, 4.32; N, 9.18.

1,3,5-Tris(pyridiniummethyl)-2,4,6-triethylbenzene Hexafluorophosphate (3). 1,3,5-Tri(bromomethyl)-2,4,6-triethylbenzene (1.00 g, 2.3 mmol) and pyridine (550 μL, 6.8 mmol) were dissolved in chloroform (70 mL), and the mixture was refluxed for 4 h. During this time, a solid white precipitate formed, which was filtered, washed with chloroform/ether, and dried in air for 24 h to give the bromide salt. Yield: 1.4 g, 2.0 mmol, 92%. ^{1}H NMR (MeOH-d_4, *J*/Hz, δ/ppm): 1.17 (t, 9H, $J = 7.4$, CH_3), 2.83 (q, 6H, $J = 7.4$, CH_2), 6.28 (s, 6H, CH_2), 8.34 (m, 6H, PyH), 8.76 (t, 3H, $J = 7.7$, PyH), 9.30 (d, 6H, $J = 7.7$, PyH). FAB-MS: $m/z = 598$ $[M - Br]^+$. Anal. Calcd for $C_{30}H_{36}Br_3N_3 \cdot 2H_2O$: C, 50.44; H, 5.64; N, 5.88. Found: C, 50.48; H, 5.52; N, 5.72. Counterion metathesis to give the hexafluorophosphate was achieved by method A described above. The white solid was isolated by filtration and washed several times with methanol and ether to yield the desired PF_6 salt. Yield: 78 mg, 0.9 mmol, 76%. ^{1}H NMR (MeCN-d_3, *J*/Hz, δ/ppm): 1.103 (t, 9H, $J = 7.6$, CH_3), 2.66 (q, 6H, $J = 7.6$, CH_2), 5.99 (s, 6H, CH_2), 8.20 (m, 6H, PyH), 8.70 (m, 9H, PyH). FAB-MS: *m*/*z* = 729 $[M - PF_6]^+$. IR (ν/cm^{-1}): 830 s (PF_6). Anal. Calcd for $C_{30}H_{36}F_{18}N_3P_3 \cdot 2H_2O$: C, 39.62; H, 4.43; N, 4.62. Found: C, 39.84; H, 4.37; N, 4.65.

1,3,5-Tris(pyridiniummethyl)benzene Hexafluorophosphate (4). 1,3,5-Tribromomethylbenzene (1.00 g, 2.80 mmol) was dissolved in CH_2Cl_2 (50 mL), and pyridine (1.00 mL, 12.3 mmol) was added dropwise and with continued stirring. A white precipitate formed almost immediately. The suspension was stirred for an hour and then filtered to give the desired product as a white powder. Yield: 1.13 g, 1.90 mmol, 68%. ^{1}H NMR (400 MHz, MeCN-d_3): 5.82 (s, 6H, $-CH_2-Py^+$), 7.87 (s, 3H, ArH), 8.02 (m, 6H, PyH*m*), 8.50 (t, $J = 7.8$ Hz, 3H, PyH*p*), 9.11 (d, $J = 7.8$ Hz, 6H, PyH*o*). The bromide salt (0.80 g, 1.35 mmol) was dissolved in CH_2Cl_2 (50 mL), and a solution of tetrabutylammonium hexafluorophosphate (5.30 g, 13.5 mmol) in CH_2Cl_2 (30 mL) was added dropwise with stirring. A white precipitate formed almost immediately. The suspension was stirred for an hour and then filtered to give the desired product as a white powder. Yield: 0.89 g, 1.13 mmol, 84%. ^{1}H NMR (400 MHz, MeCN-d_3, *J*/Hz, δ/ppm): 5.64 (s, 6H, $-CH_2-Py^+$), 7.44 (s, 3H, ArH), 8.01 (m, 6H, PyH*m*), 8.51 (t, $J = 7.9$, 3H, PyH*p*), 8.628 (d, $J = 7.9$, 6H, PyH*o*). FAB-MS: *m*/*z* 789 $[M^+ - PF_6^-]$. Anal. Calcd for $C_{24}H_{24}F_{18}N_3P_3 \cdot 2H_2O$: C, 34.92; H, 3.42; N, 5.09. Found: C, 34.62; H, 3.67; N, 4.90.

Ethylidenepyridin-3-ylamine (6). Acetyl aldehyde (2.34 g, 53 mmol) was added to a solution of 3-aminopyridine (5.0 g, 53 mmol) in dichloromethane (100 mL) and refluxed for 6 h, over which time a pale orange color formed. The solvent was removed under reduced pressure to produce the desired imine as a yellow oil. Yield: 5.0 g, 42 mmol, 79%. ^{1}H NMR ($CHCl_3$-*d*, *J*/Hz, δ/ppm): 1.1 (d, 3H, $J = 4.0$, CH_3), 6.90 (m, 1H, PyH), 7.21 (m, 1H, PyH), 7.64 (m, 1H, PyH), 8.55 (m, 1H, PyH), 8.15 (m, 1H, CH═N). FAB-MS: $m/z = 121$ $[M + H]^+$. IR (ν/cm^{-1}): 1700 *s* (CH═N).

Benzylidenepyridin-3-ylamine (7). Benzaldehyde (5.69 g, 54 mmol) was added to a solution of 3-aminopyridine (5.0 g, 54 mmol) in dichloromethane (100 mL) containing molecular sieves and refluxed for 6 h, under N_2. The solvent was removed under reduced pressure to produce the desired imine, as a colorless oil. Yield: 6.0 g, 33 mmol, 61%. ^{1}H NMR ($CHCl_3$-*d*, *J*/Hz, δ/ppm): 7.08 (m, 1H, ArH), 7.28 (m, 5H, ArH + PyH), (dd, $J = 1.6$, 7.3, 1H, ArH), 8.20 (s, 1H, CH═N), 8.30 (dd, 1H, $J = 1.5$, 5.0, PyH), 8.34 (d, 1H, $J = 2$, PyH). FAB-MS: $m/z = 182$ $[M]^+$. IR (ν/cm^{-1}): 1712 *w* (CH═N).

(4-Pentylbenzylidene)pyridin-3-ylamine (8). Benzaldehyde (5.69 g, 54 mmol) was added to a solution of 3-aminopyridine (5.0 g, 54 mmol) in dichloromethane (100 mL) containing molecular sieves and refluxed for 24 h, under N_2. The solvent was removed under reduced pressure to produce the desired imine, as a white oil. Yield: 9.0 g, 36 mmol, 66%. ^{1}H NMR ($CHCl_3$-*d*, *J*/Hz, δ/ppm): 0.84 (t, 3H, $J = 6.7$, CH_3), 1.27 (sp, 4H, $J = 3.4$, 5.1, 9.8, CH_2), 1.57 (q, 2H, $J = 7.5$, CH_2), 2.62 (t, 2H, $J = 7.0$), 7.33, 8.50 (AA′ BB′, 4H, $J = 8.1$, ArH), 7.41 (ddd, 1H, $J = 1.0$, 2.5, 9.0, PyH), 6.65 (dd, 1H, $J = 4.7$, 8.2, PyH), 8.45 (dd, 1H, $J = 4.5$, 1.0, PyH), 8.50 (d, 1H, $J = 2.7$, PyH), 8.63 (s, 1H, CH═N). FAB-MS: $m/z = 252$ $[M]^+$. IR (ν/cm^{-1}): 1725 *s* (CH═N).

Anthracen-9-ylmethylenepyridin-3-ylamine (9). Anthracene-9-carbaldehyde (5.00 g, 24 mmol) and 3-aminopyridine (2.28 g, 24 mmol) were dissolved in dichloromethane (200 mL) and refluxed for 24 h under a nitrogen atmosphere. The solvent was removed under reduced

pressure to produce dark yellow oil, which solidified after 24 h. Yield: 6.0 g, 21 mmol, 88%. ^{1}H NMR ($CHCl_3$-*d*, *J*/Hz, δ/ppm): 7.74 (m, 1H, PyH), 7.46 (m, 1H, PyH), 7.65−7.72 (m, 4H, AnH), 8.09 (m, 2H, AnH), 8.64 (m, 1H, PyH), 8.73 (s, 1H, CH), 8.75 (m, 1H, PyH), 8.83 (m, 2H, AnH), 9.76 (s, 1H, AnH). FAB-MS: m/z = 282 $[M]^+$. IR (ν/cm^{-1}): 1750 *s* (C═N). Anal. Calcd for $C_{20}H_{14}N_2$: C, 85.08; H, 5.00; N, 9.92. Found: C, 85.14; H, 4.92; N, 9.85.

Ethylpyridin-3-ylamine (10). Ethylidenepyridin-3-ylamine (**6**, 3.0 g, 25 mmol) was dissolved in methanol (70 mL), to which a slight excess of sodium borohydride (1.13 g, 30 mmol) was added slowly as a solid to the methanolic solution, and the resulting solution was stirred at room temperature for 45 min, during which time the orange solution turned yellow. 2 M hydrochloric acid was then added to destroy the excess sodium borohydride. Once the effervescence had stopped, 2 M sodium hydroxide was added until pH 9 was obtained. The yellow solution was then extracted into dichloromethane, washed three times with water (150 mL), separated, dried over magnesium sulfate, and filtered through Celite before the solvent was removed under reduced pressure, producing a yellow oil. Yield: 2.5 g, 20 mmol, 82%. ^{1}H NMR ($CHCl_3$-*d*, *J*/Hz, δ/ppm): 1.23 (t, 3H, J = 7.2, CH_3), 3.10 (q, 2H, J = 7.2, 6.3, CH_2), 4.50 (br, s, 1H, NH), 7.26 (m, 1H, PyH), 7.40 (m, 1H, PyH), 8.23 (m, 1H, PyH), 8.50 (s, 1H, PyH). EI-MS: m/z = 123 $[M]^+$. IR (ν/cm^{-1}): 2370 *w* (NH). Anal. Calcd for $C_{12}H_{12}N_2$: C, 68.82; H, 8.27; N, 22.93. Found: C, 68.34; H, 8.11; N, 22.21.

Benzylpyridin-3-ylamine (11). Benzylidenepyridin-3-ylamine (**7**, 9.5 g, 52 mmol) and sodium borohydride (4.0 g, 105 mmol) were added to methanol (100 mL), and the procedure was carried out as described for **10**. The solvent was removed under reduced pressure, and the crude product was recrystallized from CH_2Cl_2 and *n*-hexane to produce the desired product as a pale pink solid. Yield: 7.7 g, 42 mmol, 80%. ^{1}H NMR ($CHCl_3$-d_3, *J*/Hz, δ/ppm): 4.33 (s, 2H, CH_2), 4.40 (s, *br*, 1H, NH) disappears on D_2O shake, 6.87 (m, 1H, ArH), 7.20 (dd, 1H, J = 5.0, 8.0, ArH), 7.36 (m, 5H, ArH), 7.96 (dd, 1H, J = 1.0, 5.0, ArH), 8.07 (d, 1H, J = 3.0, PyH). EI-MS: m/z = 184 $[M]^+$. IR (ν/cm^{-1}): 3248 *w* (NH). Anal. Calcd for $C_{12}H_{12}N_2$: C, 78.23; H, 6.57; N, 15.21. Found: C, 78.10; H, 6.51; N, 15.18.

(4-Pentylbenzyl)pyridin-3-ylamine (12). (4-Pentylbenzylidene)-pyridin-3-ylamine (**8**, 9.5 g, 38 mmol) and sodium borohydride (4.3 g, 113 mmol) were added to methanol (100 mL), and the procedure was carried out as described for **9**. The solvent was removed under reduced pressure, and the crude product was recrystallized from CH_2Cl_2 and *n*-hexane to produce the desired product as a white solid. Yield: 8.5 g, 42 mmol, 86. ^{1}H NMR ($CHCl_3$-*d*, *J*/Hz, δ/ppm): 0.83 (t, 3H, J = 6.8, CH_3), 1.26 (sp, 4H, J = 3.5, 5.0, 9.6, CH_2), 1.53 (qt, 2H, J = 7.6, CH_2), 2.51 (t, 2H, J = 7.6, CH_2), 4.04 (br, s, 1H, NH), 4.21 (s, 2H, CH_2), 6.80 (dd, 1H, J = 4.7, 8.2, PyH), 6.98 (ddd, 1H, J = 1.0, 2.7, 9.4, PyH), 7.08, 7.16 (AA′ BB′, 4H, J = 8.0, ArH), 7.89 (dd, 1H, J = 4.5, 1.0, PyH), 7.99 (d, 1H, J = 2.7, PyH). EI-MS: m/z = 255 $[M + H]^+$. IR (ν/cm^{-1}): 3215 *w* (NH). Anal. Calcd for $C_{12}H_{12}N_2$: C, 80.27; H, 8.72; N, 11.01. Found: C, 80.46; H, 9.00; N, 11.61.

Anthracen-9-ylmethylpyridin-3-ylamine (13). Sodium borohydride (1.2 g, 32 mmol) was added to a methanolic solution of **9** (3.0 g, 11 mmol), and the mixture was stirred at room temperature for 2 h. Over this time period, the solution turned a light yellow. The solution was made acidic (pH 5) by the addition of 2 M HCl and then basic (pH 9) with 2 M NaOH. The product was extracted into CH_2Cl_2 (100 mL), washed several times with water (100 mL), dried over $MgSO_4$, and filtered to produce a yellow solution. The solvent was removed under pressure to produce a dark yellow solid. This solid was chromatographed on silica gel with CH_2Cl_2:MeOH (97:3) solution as the eluent. The solvent was removed, and the residue was recrystallized from CH_2Cl_2 and hexane, to yield the product as a yellow solid. Yield: 2.5 g, 9.0 mmol, 83%. ^{1}H NMR ($CHCl_3$-*d*, *J*/Hz, δ/ppm): 3.89 (s, br, 1H, NH), 5.17 (d, 2H, J = 4.3, CH_2), 7.11−7.13 (m, 1H, PyH), 7.21−7.24 (m, 1H, PyH), 7.50−7.59 (m, 4H, ArH), 8.07 (d, 2H, J = 8.9, AnH), 8.10 (m, 1H, PyH), 8.20 (d, 1H, J = 2.7, PyH), 8.25 (d, 2H, J = 8.7, AnH), 8.52 (s, 1H, PyH). FAB-MS: m/z = 284 $[M]^+$. IR (ν/cm^{-1}): 3215 *w* (NH). Anal. Calcd for $C_{20}H_{16}N_2$: C, 84.48; H, 5.67; N, 9.85. Found: C, 84.78; H, 5.52; N, 9.59.

1,3,5-Tris(3-(*N*-ethylamino)pyridiniummethyl)-2,4,6-triethylbenzene Bromide (14). Ethylpyridin-3-ylamine (**10**, 2.0 g, 16.0 mmol) and 1,3,5-tris(bromomethyl)-2,4,6-triethylbenzene (2.4 g, 5.4 mmol) were dissolved in chloroform (80 mL) and refluxed for 24 h. The solvent was removed under reduced pressure, and the resulting oil was placed under high vacuum, producing a white solid identified as the bromide salt. Yield: 2.5 g, 3.1 mmol, 57%. ^{1}H NMR (MeOH-d_4, *J*/Hz, δ/ppm): 0.93 (t, 9H, J = 7.3, CH_3), 1.10 (t, 9H, J = 7.0, CH_3), 2.59 (q, 6H, 7.6, CH_2), 2.69 (q, 6H, 7.6, CH_2), 4.46 (s, 6H, CH_2), 7.34−7.40 (m, 3H, ArH), 7.69 (m, 3H, J = 2.0, 9.0, ArH), 7.70 (m, 3H, ArH), 8.22 (d, 3H, J = 6.0), 8.62 (s, 3H, ArH). FAB-MS: m/z = 727 $[M\text{-}Br]^+$. Anal. Calcd for $C_{36}H_{51}Br_3N_6$: C, 53.54; H, 6.37; N, 10.41. Found: C, 53.00; H, 6.35; N, 10.28. Attempts to prepare a clean sample of the corresponding hexafluorophosphate salt were unsuccessful.

1,3,5-Tris(3-(*N*-benzylamino)pyridiniummethyl)-2,4,6-triethylbenzene Hexafluorophosphate (15). 3-(*N*-Benzylamino)pyridine (**11**, 1.5 g, 8.0 mmol) and 1,3,5-tri(bromomethyl)-2,4,6-triethylbenzene (1.2 g, 3 mmol) were dissolved in chloroform (80 mL), and the mixture was refluxed for 24 h. The solvent was removed under reduced pressure, and the resulting oil was placed under high vacuum, producing a pale orange solid identified as the bromide salt. Yield: 2.5 g, 2.5 mmol, 93%. ^{1}H NMR (MeOH-d_4, *J*/Hz, δ/ppm): 0.93 (t, 9H, J = 7.3 Hz, CH_3), 2.64 (q, 6H, J = 7.6, CH_2), 4.46 (s, 6H, CH_2), 5.92 (s, 6H, CH_2), 7.24−7.40 (m, 15H, ArH), 7.59 (dd, 3H, J = 2.0, 9.0, ArH), 7.70 (m, 3H, ArH), 8.22 (d, 3H, J = 6.0), 8.38 (s, 3H, ArH). FAB-MS: m/z = 914 $[M - Br]^+$. Anal. Calcd for $C_{30}H_{39}Br_3N_6 \cdot 4H_2O$: C, 40.43; H, 4.96; N, 11.82. Found: C, 41.06; H, 5.38; N, 12.16. Counterion metathesis to give the hexafluorophosphate was achieved by method A as described above, producing a pale blue solid which was filtered, washed with methanol/ether, and dried in air to produce the desired hexafluorophosphate salt. Yield: 800 mg, 0.7 mmol, 67%. ^{1}H NMR (MeCN-d_3, *J*/Hz, δ/ppm): 0.79 (t, 9H, J = 7.3, CH_3), 2.46 (q, 6H, J = 7.6, CH_2), 4.41 (d, 6H, J = 5.9, CH_2), 5.61 (s, 6H, CH_2), 6.35 (br, s, 3H, NH), 7.29−7.37 (m, 15H, ArH + PyH), 7.57−7.61 (m, 9H, ArH + PyH), 7.72 (s, 3H, PyH). FAB-MS: m/z = 1045 $[M - PF_6]^+$, 901 $[M - 2PF_6]^+$. IR (ν/cm^{-1}): 3225 *m*, 840 *s*, *br* (PF_6). Anal. Calcd for $C_{51}H_{57}F_{18}N_6P_3$: C, 51.52; H, 4.83; N, 7.07. Found: C, 51.63; H, 4.80; N, 7.01.

1,3,5-Tris(3-(*N*-(4-pentyl)benzylamino)pyridiniummethyl)-2,4,6-triethylbenzene Hexafluorophosphate (16). 3-(*N*-(4-Pentylbenzyl)-amino)pyridine (**12**, 1.5 g, 6.0 mmol) and 1,3,5-tri(bromomethyl)-2,4,6-triethylbenzene (868 mg, 2.0 mmol) were dissolved in chloroform (80 mL) and refluxed for 24 h. The solvent was removed under reduced pressure, and the resulting oil was placed under high vacuum, producing a pale orange solid which was identified as the bromide salt. Yield: 6.0 g, 5.0 mmol, 83%. ^{1}H NMR (MeOH-d_4, *J*/Hz, δ/ppm): 0.96 (m, 18H, CH_3), 1.50 (m, 12H, CH_2), 1.63 (m, 6H, CH_2), 2.52 (m, 6H, CH_2), 2.61 (m, 6H, CH_2), 4.27 (s, 6H, CH_2), 5.68 (s, 6H, CH_2), 7.05, 7.21 (d, AA′ BB′ 12H, J = 8.0, ArH), 7.40 (m, 3H, PyH), 7.66 (m, 3H, PyH), 8.14 (d, 3H, J = 6.0 PyH), 8.62 (s, 3H, PyH). FAB-MS: m/z = 1124 $[M - Br]^+$, 1004 $[M - 2Br]^+$. Anal. Calcd for $C_{66}H_{87}Br_3N_6$: C, 55.83; H, 7.28; N, 6.98. Found: C, 55.60; H, 7.30; N, 6.23. Counterion metathesis to give the hexafluorophosphate was achieved by method A described in the General Procedure for Counterion Metathesis section, to produce a pale blue solid which was filtered, washed with methanol/ether, and dried in air to produce the desired hexafluorophosphate salt. Yield: 2.0 g, 1.4 mmol, 87%. ^{1}H NMR (MeCN-d_3, *J*/Hz, δ/ppm): 0.88 (m, 18H, CH_3), 1.30 (m, 12H, CH_2), 1.57 (m, 6H, CH_2), 2.48 (m, 6H, CH_2), 2.57 (m, 6H, CH_2), 4.36 (s, 6H, CH_2), 5.62 (s, 6H, CH_2), 6.38 (br, s, 3H, NH), 7.10−7.22 (m, 12H, ArH + PyH), 7.50−7.60 (m, 9H, ArH + PyH), 7.83 (br, s, 3H, PyH). FAB-MS: m/z = 1256 $[M - PF_6]^+$, 1112 $[M - 2PF_6]^+$. IR (ν/cm^{-1}): 3220 *m*, 837 *s*, *br* (PF_6). Anal.

Calcd for $C_{66}H_{87}F_{18}N_6P_3$: C, 56.65; H, 6.27; N, 6.01. Found: C, 56.27; H, 6.30; N, 5.60.

1,3,5-Tris(3-(9-anthracenylmethylamino)pyridinium)-2,4,6-triethylbenzene Hexafluorophosphate (17). 1,3,5-Tri(bromomethyl)-2,4,6-triethylbenzene (400 mg, 0.9 mmol) and compound **13** (773 mg, 2.7 mmol) were refluxed in $CHCl_3$ (70 mL) for 18 h. The solvent was removed under reduced pressure, to produce the desired product as the bromide salt. Yield: 90 mg, 0.9 mmol, 77%. ^{1}H NMR (MeOH-d_4, *J*/Hz, δ/ppm): 1.04 (t, 9H, $J = 7.3$, CH_3), 3.3 (q, 6H, $J = 7.1$, CH_2), 5.25 (s, 6H, CH_2), 5.97 (s, 6H, CH_2), 7.49−7.60 (m, 12H, AnH), 7.61 (m, 3H, PyH), 7.69 (m, 3H, PyH), 8.01 (m, 9H, AnH + PyH), 8.25 (m, 6H, AnH), 8.51 (s, 3H, PyH), 8.56 (s, 3H, AnH). FAB-MS: $m/z = 954$ [M − Br]$^+$, 810 [M − Br]$^+$. IR (ν/cm^{-1}): 3207 *w* (NH). Anal. Calcd for $C_{75}H_{69}Br_3N_6 \cdot H_2O$: C, 68.65; H, 5.45; N, 6.40. Found: C, 68.30; H, 4.96; N, 5.86. Counterion metathesis to give the hexafluorophosphate salt was achieved as described for the bis(anthracenyl) species. The yellow solid was filtered and washed with MeOH and ether and dried in air for 24 h, to produce the desired hexafluorophosphate salt. Yield: 1.0 g, 0.7 mmol, 71%. ^{1}H NMR (MeCN-d_3, *J*/Hz, δ/ppm): 1.05 (t, 9H, $J = 7.3$, CH_3), 2.67 (q, 6H, $J = 7.1$, CH_2), 5.24 (d, 6H, $J = 4.0$, CH_2), 5.80 (s, 6H, CH_2), 6.01 (br, 3H, NH) disappears on D_2O shake, 7.54−7.68 (m, 21H, AnH + PyH), 8.10 (s, 3H, AnH), 8.16 (d, 6H, $J = 7.7$, AnH), 8.28 (b, 6H, $J = 8.4$, PyH), 8.67 (s, 3H, PyH). FAB-MS: $m/z = 1343$ [M − PF$_6$]$^+$, 1197 [M − 2PF$_6$]$^+$. IR (ν/cm^{-1}): 3392 *m* (NH), 854 *s* (PF_6). Anal. Calcd for $C_{75}H_{69}N_6F_{18}P_3 \cdot H_2O$: C, 59.76; H, 4.75; N, 5.58. Found: C, 59.61; H, 4.21; N, 5.31.

General Procedure for the Synthesis of Compounds 18a−c. The three bis(anthracenyl) isomers were synthesized in the same way. The appropriate dibromoxylene (0.500 g, 1.9 mmol) and anthracen-9-yl methylpyridin-3-ylamine (1.08 g, 3.8 mmol) were dissolved in CH_2Cl_2 (100 mL) and refluxed for 18 h. During this time, a precipitate appeared in all three cases. The solid was filtered, washed with CH_2Cl_2 and ether, and dried in air for 24 h.

α,α′-Bis(3-(9-anthracenylmethylamino)pyridinium)-*ortho*-xylene Hexafluorophosphate (18a). The procedure was carried out as described above. The pale yellow solid obtained after the metathesis was filtered, washed with ether, and dried in air for 24 h (100 mg, 0.1 mmol, 87%). ^{1}H NMR (MeOH-d_4, *J*/Hz, δ/ppm): 5.24 (s, 4H, CH_2), 6.00 (s, 4H, CH_2), 6.05−7.3 (m, 2H, PyH), 7.46−7.56 (m, 10H, AnH + BzH), 7.66−7.76 (m, 4H, BzH + PyH), 8.07 (m, 6H, AnH + PyH), 8.26 (d, $J = 8.0$, 4H, AnH), 8.38 (s, 2H, AnH), 8.56 (*s*, 2H, PyH). FAB-MS: $m/z = 753.1$ [M − Br]$^+$, 671.1 [M − 2Br]$^+$. IR (ν/cm^{-1}): 3384 *w* (NH). Anal. Calcd for $C_{48}H_{40}Br_2N_4 \cdot 2H_2O$: C, 66.37; H, 5.11; N, 6.45. Found: C, 66.56; H, 5.05; N, 6.55. Counterion metathesis to give the hexafluorophosphate salt was achieved by stirring a solution of the bromide salt (100 mg, 0.12 mmol) in CH_2Cl_2 (50 mL) with a solution of $NaPF_6$ (121 mg, 0.7 mmol) in water (50 mL). After 1 h, a precipitate formed that was filtered, washed with methanol and diethyl ether, and dried in air for 24 h (103 mg, 0.10 mmol, 89%). ^{1}H NMR (MeCN-d_3, *J*/Hz, δ/ppm): 5.19 (d, 4H, $J = 4.2$, CH_2), 5.72 (s, 4H, CH_2), 5.97 (br, 2H, NH) disappears on D_2O shake, 7.46−7.56 (m, 12H, AnH + BzH + PyH), 7.66−7.76 (m, 4H, BzH + PyH), 8.07 (m, 6H, AnH + PyH), 8.26 (d, $J = 8.0$, 4H, AnH), 8.38 (s, 2H, AnH), 8.56 (s, 2H, PyH). FAB-MS: $m/z = 962$ [M]$^+$, 817 [M − PF$_6$]$^+$, 672 [M − 2PF$_6$]. IR (ν/cm^{-1}): 3656 *w* (NH), 3561 *w* (NH), 833 *s* (PF_6). Anal. Calcd for $C_{48}H_{40}F_{12}N_4P_2$: C, 59.88; H, 4.19; N, 5.82. Found: C, 59.58; H, 4.07; N, 5.83.

α,α′-Bis(3-(9-anthracenylmethylamino)pyridinium)-*meta*-xylene Hexafluorophosphate (18b). The procedure was carried out as described above. The pale orange/yellow solid obtained after the metathesis was filtered, washed with ether, and dried in air for 24 h. Yield: 98 mg, 0.1 mmol, 85%. ^{1}H NMR (MeOH-d_4, *J*/Hz, δ/ppm): 5.14 (s, 4H, CH_2), 5.68 (s, 4H, CH_2), 7.34−7.43 (m, 8H, AnH + PyH + BzH), 7.48 (m, 4H, PyH), 7.85 (m, 4H, PyH), 7.61 (m, 1H, BzH), 7.95 (m, 4H, AnH), 8.14 (m, 5H, AnH + BzH), 8.44 (m, 4H, AnH + PyH). FAB-MS: $m/z = 753$ [M − Br]$^+$, 671 [M − 2Br]$^+$. IR (ν/cm^{-1}): 3160 *w* (NH). Anal. Calcd for $C_{48}H_{40}Br_2N_4 \cdot 2H_2O$: C, 66.37; H, 5.11; N, 6.45. Found: C, 66.60; H, 4.65; N, 6.22. Counterion metathesis to give the hexafluorophosphate salt was achieved by stirring a solution of the bromide salt (100 mg, 0.12 mmol) in CH_2Cl_2 (50 mL) with a solution of $NaPF_6$ (121 mg, 0.7 mmol) in water (50 mL). After 1 h, a precipitate formed that was filtered, washed with methanol and diethyl ether, and dried in air for 24 h (109 mg, 0.11 mmol, 92%). ^{1}H NMR (MeCN-d_3, *J*/Hz, δ/ppm): 5.18 (d, 4H, $J = 4.2$, CH_2), 5.71 (s, 4H, CH_2), 5.99 (br, 2H, NH) disappears on D_2O shake, 7.30−7.32 (m, 2H, PyH), 7.50−7.59 (m, 10H, AnH + BzH + PyH), 7.67−7.69 (m, 4H, BzH + PyH), 7.70 (m, 2H, BzH), 8.02 (s, 2H, AnH), 8.11 (d, 4H, $J = 8.0$, AnH), 8.23 (d, 4H, $J = 8.0$, AnH), 8.62 (s, 2H, PyH). FAB-MS: $m/z = 962$ [M]$^+$, 817 [M − PF$_6$]$^+$, 671 [M − 2PF$_6$]$^+$. IR (ν/cm^{-1}): 3411 *w*, 3422 *w* (NH), 844 *s* (PF_6). Anal. Calcd for $C_{48}H_{40}F_{12}N_4P_2$: C, 59.88; H, 4.19; N, 5.82. Found: C, 59.72; H, 4.06; N, 5.72.

α,α′-Bis(3-(9-anthracenylmethylamino)pyridinium)-*para*-xylene Hexafluorophosphate (18c). The procedure was carried out as described above. The pale orange/yellow solid obtained after the metathesis was filtered, washed with ether, and dried in air for 24 h. Yield: 98 mg, 0.1 mmol, 85%. ^{1}H NMR (MeOH-d_4, *J*/Hz, δ/ppm): 5.27 (s, 4H, CH_2), 5.78 (s, 4H, CH_2), 7.48−7.57 (m, 8H, AnH + PyH), 7.62 (s, 4H, BzH), 7.67−7.84 (m, 4H, AnH + PyH), 8.11 (m, 4H, AnH), 8.50 (m, 6H, AnH + PyH), 8.42 (s, 2H, PyH), 8.58 (s, 2H, AnH). FAB-MS: $m/z = 753$ [M − Br]$^+$, 671 [M − 2Br]$^+$. IR (ν/cm^{-1}): 3196 *w* (NH). Anal. Calcd for $C_{48}H_{40}Br_2N_4$: C, 69.24; H, 4.84; N, 6.73. Anal. Calcd for $C_{48}H_{40}Br_2N_4 \cdot 2H_2O$: C, 66.37; H, 5.11; N, 6.45. Found: C, 66.32; H, 5.29; N, 6.28. Counterion metathesis to give the hexafluorophosphate salt was achieved by stirring a solution of the bromide salt (100 mg, 0.12 mmol) in CH_2Cl_2 (50 mL) with a solution of $NaPF_6$ (121 mg, 0.7 mmol) in water (50 mL). After 1 h, a precipitate formed that was filtered, washed with methanol and diethyl ether, and dried in air for 24 h (86 mg, 0.09 mmol, 75%). ^{1}H NMR (MeCN-d_3, *J*/Hz, δ/ppm): 5.21 (d, 4H, $J = 4.3$, CH_2), 5.65 (s, 4H, CH_2), 5.96 (br, 2H, NH) disappears on D_2O shake, 7.49−7.61 (m, 12H, AnH + PyH), 7.72 (s, 2H, AnH), 7.73 (d, 2H, $J = 1.2$, PyH), 8.04 (d, 2H, $J = 1.5$, BzH), 8.11 (d, 2H, $J = 1.5$, BzH), 8.13 (d, 4H, $J = 8.6$, AnH), 8.25 (d, 4H, $J = 8.6$, AnH), 8.62 (s, 2H, PyH). FAB-MS: $m/z = 961$ [M]$^+$, 817 [M − PF$_6$]$^+$, 671 [M − 2PF$_6$]$^+$. IR (ν/cm^{-1}): 3424 *w* (NH), 838 *s* (PF_6). Anal. Calcd for $C_{40}H_{48}F_{12}N_4P_2$: C, 59.88; H, 4.19; N, 5.82. Found: C, 59.71; H, 4.29; N, 5.79.

***N*-Benzyl-3-(9-anthracenylmethylamino)pyridinium Hexafluorophosphate (19).** Benzyl bromide (500 mg, 2.9 mmol) and compound **13** (833 mg, 2.9 mmol) were refluxed in $CHCl_3$ (70 mL) for 18 h. The solvent was removed under reduced pressure, to produce the desired product as the bromide salt; this was converted to the PF_6 salt as described for **17**. Yield: 150 mg, 2.8 mmol, 88%. ^{1}H NMR (MeOH-d_4, *J*/Hz, δ/ppm): 5.32 (s, 2H, CH_2), 5.61 (s, 2H, CH_2), 7.47−7.52 (m, 4H, BzH), 7.52−7.64 (m, 5H, AnH + PyH), 7.72−7.75 (m, 2H, PyH), 8.03 (m, 1H, BzH), 7.47−7.52 (m, 3H, BzH), 8.33 (m, 2H, BzH), 8.66 (s, 1H, AnH). FAB-MS: $m/z = 375$ [M − Br]$^+$. IR (ν/cm^{-1}): 3330 *m* (NH). Anal. Calcd for $C_{27}H_{23}N_2Br$: C, 71.21; H, 5.09; N, 6.15. Found: C, 70.83; H, 4.52; N, 6.38. Counterion metathesis to give the hexafluorophosphate salt was achieved by the same procedure described for compounds **18**. ^{1}H NMR (MeCN-d_3, *J*/Hz, δ/ppm): 5.24 (d, 2H, $J = 4.0$, CH_2), 5.61 (s, 2H, CH_2), 5.92 (br, 1H, NH) disappears on D_2O shake, 7.47−7.52 (m, 4H, BzH), 7.52−7.64 (m, 5H, AnH + PyH), 7.72−7.75 (m, 2H, PyH), 8.03 (m, 1H, BzH), 7.47−7.52 (m, 3H, BzH), 8.33 (m, 2H, BzH), 8.66 (s, 1H, AnH). FAB-MS: $m/z = 375$ [M − PF$_6$]$^+$. IR (ν/cm^{-1}): 3433 *m*, 831 *s* (PF_6). Anal. Calcd for $C_{27}H_{23}N_2F_6P$: C, 62.31; H, 4.64; N, 5.37. Found: C, 61.71; H, 4.45; N, 5.38.

X-ray Crystallography. Details of general crystallographic procedures in our laboratory have been published previously.[49] Structures

(49) Calleja, M.; Johnson, K.; Belcher, W. J.; Steed, J. W. *Inorg. Chem.* **2001**, *40*, 4978−4985.

were solved and refined using the programs SHELXS-97[50] and SHELXL-97,[51] respectively. The program X-Seed[52] was used as an interface to the SHELX programs and to prepare the figures.

Crystal data for **2b**·3PF_6·CH_2Cl_2·0.5H_2O·0.5MeOH: $C_{31.5}H_{44}Cl_2F_{18}N_6OP_3$, M = 1028.54, monoclinic, space group $P2_1/c$ (No. 14), a = 21.801(4), b = 11.741(2), c = 18.512(4) Å, β = 113.781(3)°, V = 4336.3(15) Å^3, Z = 4, D_c = 1.575 g/cm^3, F_{000} = 2096, Nonius Kappa CCD diffractometer, Mo Kα radiation, λ = 0.71073 Å, T = 120(2) K, $2\theta_{max}$ = 50.0°, 16 725 reflections collected, 7471 unique (R_{int} = 0.1009). Final GOF = 1.138, R1 = 0.1348, wR2 = 0.2582, R indices based on 4561 reflections with $I > 2\sigma(I)$ (refinement on F^2), 564 parameters, 0 restraints. Lp and absorption corrections applied, μ = 0.374 mm^{-1}.

Crystal data for **2b**·3Br·CH_2Cl_2: $C_{31}H_{41}Br_3Cl_2N_6$, M = 808.33, monoclinic, space group $P2_1/c$ (No. 14), a = 21.047(4), b = 12.394(3), c = 13.721(3) Å, β = 101.324(3)°, V = 3509.4(12) Å^3, Z = 4, D_c = 1.530 g/cm^3, F_{000} = 1632, Nonius Kappa CCD, Mo Kα radiation, λ = 0.71073 Å, T = 120(2) K, $2\theta_{max}$ = 52.0°, 11 460 reflections collected, 6179 unique (R_{int} = 0.1060). Final GOF = 1.009, R1 = 0.0654, wR2 = 0.1286, R indices based on 3990 reflections with $I > 2\sigma(I)$ (refinement on F^2), 385 parameters, 0 restraints. Lp and absorption corrections applied, μ = 3.631 mm^{-1}.

Crystal data for **2c**·3Br·3MeOH: $C_{33}H_{51}Br_3N_6O_3$, M = 819.53, monoclinic, space group $P2_1/c$ (No. 14), a = 9.9283(3), b = 23.4328(8), c = 16.0910(3) Å, β = 95.029(2)°, V = 3729.13(18) Å^3, Z = 4, D_c = 1.460 g/cm^3, F_{000} = 1680, Nonius Kappa CCD diffractometer, Mo Kα radiation, λ = 0.71073 Å, T = 100(2) K, $2\theta_{max}$ = 55.0°, 26 967 reflections collected, 8506 unique (R_{int} = 0.0598). Final GOF = 1.021, R1 = 0.0371, wR2 = 0.0675, R indices based on 6662 reflections with $I > 2\sigma(I)$ (refinement on F^2), 440 parameters, 0 restraints. Lp and absorption corrections applied, μ = 3.285 mm^{-1}.

Crystal data for **3**·3Br·EtOH: $C_{32}H_{42}Br_3N_3O$, M = 724.42, orthorhombic, space group $P2_12_12_1$ (No. 19), a = 10.1837(3), b = 14.8317(5), c = 22.35450(10) Å, V = 3376.46(15) Å^3, Z = 4, D_c = 1.425 g/cm^3, F_{000} = 1472, Kappa CCD, Mo Kα radiation, λ = 0.71073 Å, T = 100(2) K, $2\theta_{max}$ = 55.0°, 18 283 reflections collected, 7505 unique (R_{int} = 0.0739). Final GOF = 1.050, R1 = 0.0502, wR2 = 0.1098, R indices based on 6786 reflections with $I > 2\sigma(I)$ (refinement on F^2), 357 parameters, 0 restraints. Lp and absorption corrections applied, μ = 3.612 mm^{-1}. Absolute structure parameter = 0.459(13), racemic twin model adopted.

Crystal data for **3**·3Br·4.5MeOH: $C_{34.5}H_{53}Br_3N_3O_{4.50}$, M = 818.53, triclinic, space group P-1, a = 11.8589(2), b = 16.2547(3), c = 19.7964(4) Å, α = 84.524(8), β = 77.220(9), γ = 86.894(8)°, V = 3702.34(12) Å^3, Z = 4, D_c = 1.468 g/cm^3, F_{000} = 1682, T = 120(2) K, $2\theta_{max}$ = 50.0°, 23 784 reflections collected, 19 297 unique (R_{int} = 0.0959). Final GOF = 1.017, R_1 [$F^2 > 2\sigma(F^2)$] 0.0632, wR_2 (all data) 0.1785, R_1 index based on 8579 reflections with $I > 2\sigma(I)$ (refinement on F^2), 782 parameters, 0 restraints. Lp and absorption corrections applied, μ = 3.309 mm^{-1}.

Crystal data for **17**·MeOH·2MeCN: $C_{80}H_{77}F_{18}N_8OP_3$, M 1601.41 g mol^{-1}, triclinic, space group P-1, a = 9.890(2), b = 17.600(4), c = 22.450(5) Å, α = 104.40(3), β = 97.60(3), γ = 91.30(3)°, V = 3745.4(13) Å^3, Z = 2, μ = 0.177 mm^{-1}, T = 120 K, reflections measured 17 493, unique data 10 301, parameters 984, R_1 [$F^2 > 2\sigma(F^2)$] 0.1881, wR_2 (all data) 0.3269. Crystals proved to be very difficult to obtain, and the best sample proved to be extremely weakly diffracting and showed evidence of twinning. As a result, the overall precision of the structure is extremely poor; however, the location of the anions and overall molecular conformation are unambiguous. Loose ISOR restraints (0.02 Å^2) were applied to C and N atom anisotropic displacement parameters to stabilize the refinement.

Acknowledgment. This work was supported by EPSRC studentships (to K.J.W. and D.R.T.) and a King's College postdoctoral fellowship (W.J.B.). We thank the EPSRC and King's College London for funding of the diffractometer system, Dr. L. J. Barbour for the program X-Seed[52] used in the X-ray structure determinations, and Dr. Peter Gans for the program HypNMR[32] used in the binding constant analyses.

Supporting Information Available: CIF files for **2b**·3PF_6·CH_2Cl_2·0.5H_2O·0.5MeOH, **2b**·3Br·CH_2Cl_2, **2c**·3Br·3MeOH, **3**·3Br·EtOH, **3**·3Br·4.5MeOH, **17**·MeOH·2MeCN. This material is available free of charge via the Internet at http://pubs.acs.org.

JA034921W

(50) Sheldrick, G. M. *Acta Crystallogr., Sect. A* **1990**, *46*, 467.
(51) Sheldrick, G. M. University of Göttingen, 1997.
(52) Barbour, L. J. *J. Supramol. Chem.* **2001**, *1*, 189−191.
(53) Frassineti, C.; Ghelli, S.; Gans, P.; Sabatini, A.; Moruzzi, M. S.; Vacca, A. *Anal. Biochem.* **1995**, *34*, 374−382.